Supplementary Information (SI) for Catalysis Science & Technology.
This journal is © The Royal Society of Chemistry 2026

Supporting Information

CO_2 mediated direct *N*-formylation of nitro compounds by metal-organic framework node-supported cobalt(II) catalyst

Swapnaneel Sarmah,† Chhaya Thadhani,† Aditya Kumar, Kuntal Manna*

[a]Department of Chemistry, Indian Institute of Technology Delhi, Hauz Khas,
New Delhi 110016, India

*Email: kmanna@chemistry.iitd.ac.in

Table of contents

1. **General experiment** S2-S3
2. **Synthesis and characterization of UiO-67 and UiO-67-CoH** S3-S7
3. **Catalytic reactions with UiO-67-CoH** S7-S15
4. **Kinetic studies** S16
5. **X-ray absorption spectroscopic analysis** S17-S19
6. **DFT calculations** S20-S35
7. **XPS analysis** S36-S38
8. **Characterization of the *N*-formylated products** S39-S48
9. **References** S50-S51

1. General experiment. All the experiments were performed under inert conditions inside the glovebox, except if any case was demonstrated. All the solvents were purchased from Finar and used without further purification. Tetrahydrofuran was dried with calcium hydride followed by distillation over Na/benzophenone. All the reagents are commercially available and used directly as received. 4,4'-Biphenyldicarboxylic acid was purchased from Alfa Aesar, and $ZrCl_4$ was purchased from Sigma Aldrich. Thermogravimetric analysis (TGA) was performed on a PerkinElmer TGA7 system on well-ground samples in a flowing nitrogen atmosphere with a heating rate of 10 °C/min with a range of 40-800 °C. Room temperature powder X-ray diffraction data were collected on a Bruker Advance diffractometer using Ni-filtered Cu Kα radiation ($\lambda = 1.5406$ Å). Data were collected with a step size of 0.05° and at count time of 1s per step over the range $4° < 2\theta < 70°$. The experimental and simulated PXRD patterns are in good agreement, indicating the monophasic nature of the bulk samples. For powder X-ray diffraction measurement of MOFs, a moist sample was mounted on a PXRD groove. After catalysis, UiO-Co was recovered after centrifugation and stored in THF. Just before the PXRD measurement, the THF was removed, and the moist sample was mounted on a PXRD groove. The catalysis was carried out without any mechanical stirring, and the recovered MOF was not dried before the measurement of PXRD to prevent any mechanical degradation and pore collapse of the MOF. For the product analysis using GC-MS, the chromatographic conditions were as follows: He was used as the carrier gas with a flow rate of 1 mL min^{-1}, an injection volume of 5.0 μL, an initial column oven temperature of 100 °C which was gradually increased to 250 °C at a rate of 5 °C min^{-1} and a detector temperature of 250 °C. ICP-OES measurements were conducted using an Agilent 5110 ICP-OES with data analysis performed using a Dichroic Spectral Combiner (DSC). Samples were diluted in a 5% HNO_3 matrix and analyzed using a six-point calibration curve ranging from 0.1 ppm to 20 ppm with the correlation coefficient >0.9990 for all the analytes. All the formylation reactions were done using 100 mL Parr pressure vessels (4793 (VGR)-T-SS-3000-DVD). The vessel was pressurized directly from a CO_2 gas tank using a gauge (0-3000 psi displayed, 0-200 bar). The chemical state of transition elements was analyzed with X-ray photoelectron spectroscopy (XPS) using a PHI 5000 VersaProbe III spectrometer with an Al-Kα ($h\nu = 1486.6$ eV) X-ray source. MOF samples were vacuum dried at room temperature before being analysed in an ultra-high vacuum environment. Surface area and pore volume were measured using a BELLSORP MAX II high-performance gas and vapor adsorption system, equipped with three microporous ports. For BET surface area measurement, the MOF sample was dried via a freezedrying method, which involved first soaking the MOF with benzene, followed by freezing the slurry at -10 °C and then slowly drying it under vacuum at the same temperature. The morphology and the chemical composition of the MOFs were examined using a Zeiss FE-SEM Ultra Plus55 field emission scanning microscope (FE-EM) operating at 20 kV. After vacuum drying, a very small amount of the powder samples of MOF (1-2 mg) were dispersed on the carbon tape for FE-SEM imaging. Infra-red (IR) spectra of samples were recorded with FT-IR Spectrometer (MS-632). First, the MOF samples were vacuum dried at 100 °C to remove any residual moisture before being transferred into the glovebox. A KBr pellet of the powdered sample was then prepared and kept under inert conditions while IR spectra were recorded in a nitrogen atmosphere. EPR spectra were recorded on a Bruker A300-9.5/12/S/W spectrometer operating in the X-band region, and the spectra were simulated using Bruker EPR Simfonia software. The ESI-mass spectra data was recorded on a Waters Xevo-G2XQTOF Micro-TOF QII instrument.

2. Synthesis and characterization of UiO-67, UiO-67-CoCl and UiO-67-CoH.

2.1 Synthesis of UiO-67.[1] UiO-67 MOF was synthesized by a solvothermal reaction between $ZrCl_4$ and biphenyl-4,4'-dicarboxylic acid (H_2bpdc). First, $ZrCl_4$ (16.75 mg, 0.0718 mmol) was dissolved in 1.25 mL DMF, and then 0.125 mL HCl was added. After that, the mixture was sonicated at room temperature in a 5 mL vial until a clear solution was formed. Additionally, biphenyl-4,4'-dicarboxylic acid (22.5 mg, 0.0928 mmol) was dissolved in 2.5 mL of DMF and sonicated. The two solutions were then mixed, producing a white colored mixture. The resultant mixture was then placed in a pre-heated oven at 80 °C for 20 h. After cooling to room temperature, the white crystalline solid, UiO-67 MOF was collected via centrifugation, which was then washed with DMF and THF for several times. The final product was then stored in THF at room temperature.

2.2 Synthesis of UiO-67-CoCl.[2] Inside a glovebox, UiO-67 (0.016 g, 0.0075 mmol) was suspended in 1 mL of THF and then treated with *n*-BuLi (27 µL, 1.65 M in cyclohexane). The mixture was stirred at room temperature for 2 h to initiate the post-synthetic metalation of the MOF. Excess *n*-BuLi was removed by repeated washing with THF. Additionally, a 15 mL THF solution containing $CoCl_2.6H_2O$ (0.014 g, 0.058 mmol) was added, and the reaction mixture was stirred for 6 h at room temperature to furnish Zr-node supported cobalt chloride (UiO-67-CoCl) as a blue crystalline solid, which was then thoroughly washed with THF.

2.3 Synthesis of UiO-67-CoH. Inside a glovebox, UiO-67-CoCl (0.014 g, 0.006 mmol) was first dispersed in THF and then treated with $NaEt_3BH$ (21 µL, 1 M in toluene). The mixture was stirred at room temperature for 1 h, initiating the halide-hydride exchange reaction and giving UiO-67-CoH as a black solid. The resulting product was then thoroughly washed with THF multiple times and stored in THF within the glovebox. Thermogravimetric analysis (TGA) suggested a 30% solvent weight loss for UiO-67-CoH and inductively coupled plasma spectroscopy (ICP-OES) revealed iron loading of 45% relative to the μ_3-OH groups of the digested MOF corresponding to the molecular formula of $Zr_6O_{44}C_{84}H_{48}Li_{2.2}Co_{1.8}H_{1.8}$.

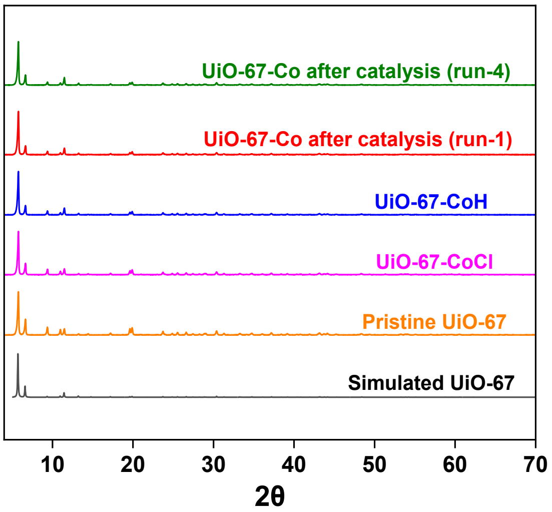

Figure S1. PXRD patterns of simulated UiO-67 MOF (black), freshly prepared pristine UiO-67 (orange), UiO-67-CoCl (magenta), UiO-67-CoH (blue), UiO-67-Co after run-1 of catalysis (red) and UiO-67-Co after run-4 of catalysis (olive).

2.4 Synthesis of UiO-66-CoH. Firstly, a solvothermal reaction was carried out between benzene-1,4-dicarboxylic acid (0.05 g, 0.300 mmol) in 1.5 mL DMF and zirconium(IV) chloride (0.069 g, 0.296 mmol) in 1.5 mL DMF in a teflon-lined hydrothermal autoclave in a preheated oven at 120 °C for 24 h to generate a white crystalline solid, UiO-66 MOF. The synthesized MOF was then isolated, washed three times with DMF and with THF. Following this, for post-synthetic metalation, UiO-66 MOF (0.013 g, 0.0078 mmol) in THF was treated with *n*-BuLi (28 µL, 1.65 M in cyclohexane) and stirred for 2 h inside a glovebox. Excess *n*-BuLi was removed by washing followed by the addition of $CoCl_2.6H_2O$ (0.014 g, 0.058 mmol) in 15 mL THF. The mixture was stirred for 6 hours to afford a blue crystalline solid, UiO-66-CoCl. Next, UiO-66-CoCl (0.011 mg, 0.0060 mmol) in THF was reacted with $NaEt_3BH$ (19 µL, 1 M in toluene) and stirred for 1 h, initiating halide-hydride exchange to yield UiO-66-CoH, a black solid which was then washed and stored in THF within the glovebox. ICP-OES confirmed 40% cobalt loading relative to μ_3-OH groups corresponding to the molecular formula of $Zr_6O_{32}C_{48}H_{24}Li_{2.4}Co_{1.6}H_{1.6}$.

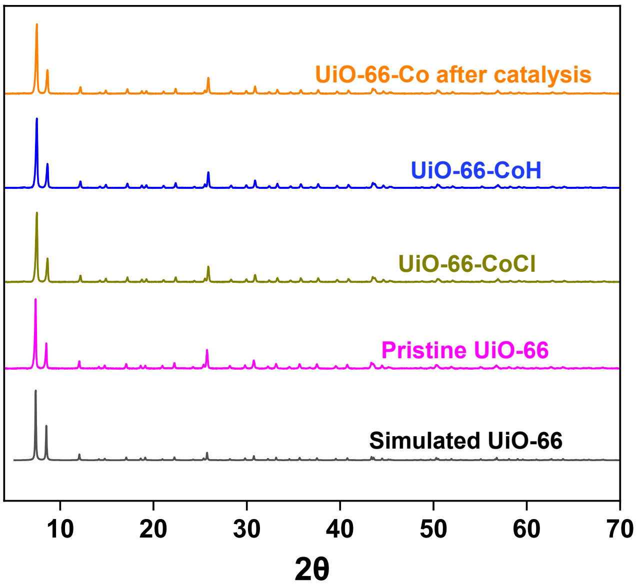

Figure S2. PXRD patterns of simulated UiO-66 MOF (black), freshly prepared pristine UiO-66 (magenta), UiO-66-CoCl (olive), UiO-66-CoH (dark yellow), UiO-66-Co after run 1 of catalysis (orange).

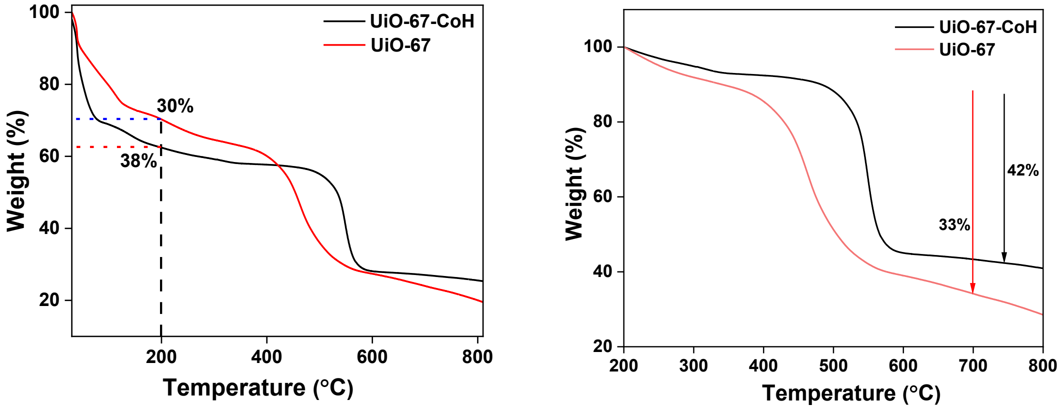

Figure S3. a) TGA curve of freshly prepared UiO-67 and UiO-67-CoH. A solvent weight loss of 38% in UiO-67 (red) and 30% in UiO-67-CoH (blue) was observed from 40 °C to 200 °C. b) TGA curve of freshly prepared UiO-67 (red) and UiO-67-CoH (blue) from 200 °C to 800 °C. The increased weight of metalated MOFs is due to the presence of cobalt within the MOF.

Table S1. Determination of defects in UiO-67 and UiO-67-CoH by TGA analysis.

		Solvent%	**Ligand%**	**Residue%**
UiO-67	Calculated	-	65	35
	TGA	38	34	28
	Corrected	-	67	33
UiO-67-CoH	Calculated	-	61	39
	TGA	30	43	27
	Corrected	-	58	42

Theoretical Calculations:

a) 1 mole of $Zr_6O_4(OH)_4(C_{14}H_8O_4)_6$ = 6 moles of ZrO_2
2120.64 g of $Zr_6O_4(OH)_4(C_{14}H_8O_4)$ = (739.32/2120.64)*100 = 34.86% ~ 35% of residue
% Ligand = (100-35) % = 65%

b) 1 mole of $Zr_6O_4(OCoH)_{1.8}(OLi)_{2.2}(C_{14}H_8O_4)_6$ = 6 moles of ZrO_2 and 1.8 mole of CoO
2239.77 g of $Zr_6O_4(OCoH)_{1.8}(OLi)_{2.2}(C_{14}H_8O_4)_6$ = (874.194/2239.77)*100 = 39% residue
% Ligand = (100-39) % = 61 %

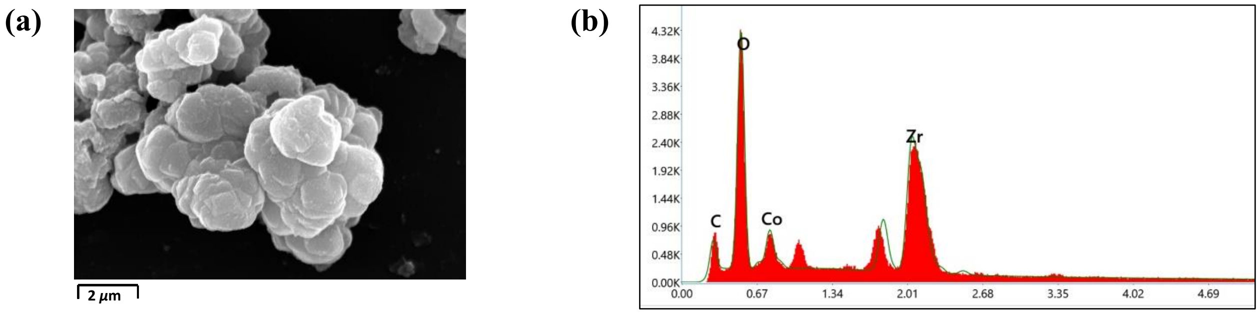

Figure S4. a) SEM image and b) SEM-EDX analysis of UiO-67-CoH. SEM image revealed octahedral-shaped UiO-67-CoH particles with an average size of 235 nm.

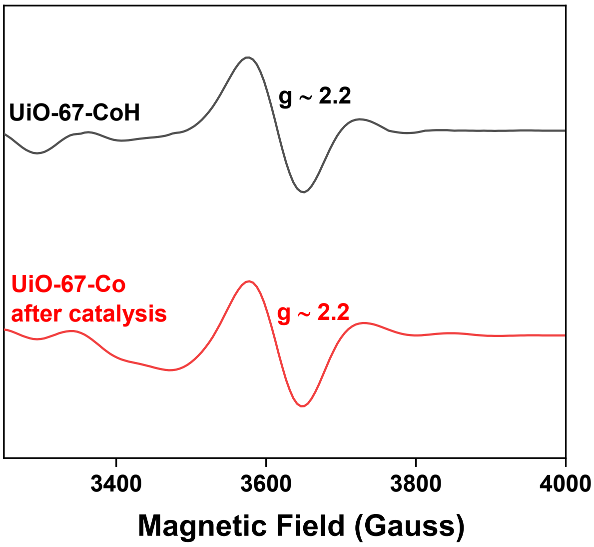

Figure S5. Room temperature X-band EPR spectra of solid UiO-67-CoH and UiO-67-Co after catalysis.[3]

3. Catalytic reactions with UiO-67-CoH.

3.1 General procedure for *N*-formylation of nitro compounds catalysed by UiO-67-CoH.

Inside the glovebox, UiO-67-CoH (0.75 mol% Co), was initially dissolved in 3 mL of solvent and transferred into a glass liner. Then various nitro substrates (1.3 mmol) along with phenylsilane (2.5 equiv.) were added to the glass liner. Following this, the liner was carefully placed inside a high-pressure Parr reactor and sealed properly. The sealed Parr reactor was then taken out from the glovebox and purged with CO_2 for 3 times. Then the reactor was pressurized to 5-15 bar CO_2 and subjected to heating at 100-140 °C for a period of 24 to 48 h without any mechanical stirring. After the completion of the reaction, the reactor was cooled to room temperature, and the pressure was released gently. The reaction mixture was then centrifuged to separate out the solid MOF, and the crude products were then analysed using GC-MS. Conversion of the reactant was analyzed by GC-MS using area-percent method and yield of the product was determined by GC using mesitylene as an internal standard.

3.2 A Typical procedure for UiO-67-CoH catalyzed *N*-formylation of *p*-nitrotoluene.

p-Nitrotoluene was chosen as the ideal substrate for carrying out the *N*-formylation reaction.

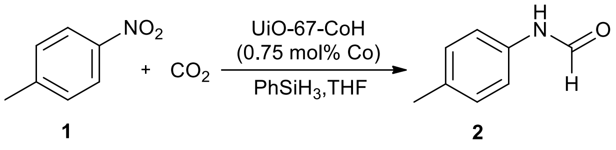

Inside the glovebox, UiO-67-CoH (0.75 mol% of Co) in 3mL of THF was transferred into a glass liner. To this, *p*-nitrotoluene (1.3 mmol) and phenylsilane (2.5 equiv.) were added. The glass liner was then placed inside a high-pressure Parr reactor and subsequently sealed. The reactor was then taken out of the glovebox and purged 3 times with CO_2. It was then pressurized to 10 bar of CO_2 and heated at 120 °C for 36 h without any mechanical stirring. After the completion of reaction, the reactor was cooled to room temperature, and the pressure was released gradually. The MOF was then separated from the reaction mixture by centrifugation. Conversion of the reactant was analyzed by GC-MS using area-percent method and yield of the product was determined by GC using mesitylene as the internal standard. After completion of the reaction, the combined organic extracts were concentrated in vacuo followed by column chromatography using hexane and ethyl acetate (5:1) as an eluent to yield *N*-*p*-tolylformamide product.

Table S2. Optimization of reaction conditions for *N*-formylation of *p*-nitrotoluene catalyzed by UiO-67-CoH.[a]

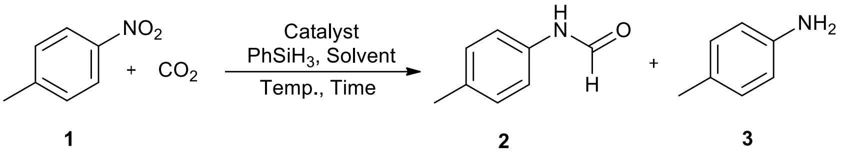

Entry	Reductant (equiv.)	Pressure (bar)	Temperature (° C)	Time (h)	Solvent	% Conversion of **1**[b]	% Yield of **2**[c]
1.	$PhSiH_3$ (1.5)	5	100	24	THF	47	18
2.	$PhSiH_3$ (1.5)	5	120	24	THF	53	21
3.	$PhSiH_3$ (1.5)	10	120	24	THF	58	32
4.	$PhSiH_3$ (1.5)	10	120	36	THF	65	49
5.	$PhSiH_3$ (1.5)	10	120	48	THF	72	53
6.	$PhSiH_3$ (2.0)	10	120	36	THF	84	78
7.	**$PhSiH_3$ (2.5)**	**10**	**120**	**36**	**THF**	**99**	**92**
8.	$PhSiH_3$ (2.5)	15	120	36	THF	99	86
9.	$PhSiH_3$ (2.5)	10	140	36	THF	80	75
10.	$PhSiH_3$ (3.0)	10	120	36	THF	99	83
11.	$PhSiH_3$ (2.5)	10	120	48	THF	99	81
12.	$PhSiH_3$ (2.5)	10	120	36	Toluene	74	72
13.	$PhSiH_3$ (2.5)	10	120	36	1,4-Dioxane	84	79
14.	Ph_2SiH_2 (2.5)	10	120	36	THF	66	54
15.	$(OEt)_2MeSiH$ (2.5)	10	120	36	THF	58	47
16.[d]	$PhSiH_3$ (2.5)	10	120	36	THF	76	52
17.	H_2	10	120	36	THF	19	0

[a]Reaction conditions: 1.3 mmol of *p*-nitrotoluene**,** UiO-67-CoH (12 mg, 0.75 mol% of Co) and 3 mL of solvent. [b]Conversion of *p*-nitrotoluene was determined by GC-MS using area-percentage method. [c]Yield of *N*-*p*-tolylformamide was determined by GC using mesitylene as an internal standard. [d]UiO-67-CoH (4 mg, 0.25 mol% of Co).

Table S3. Control experiments for *N*-formylation of *p*-nitrotoluene.[a]

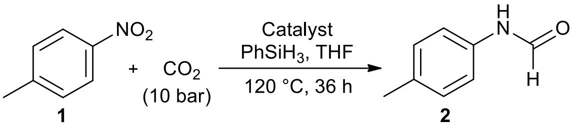

Entry No.	Catalyst	% Conversion of 1[c]	% Yield of 2[d]
1	UiO-67-CoH	**99**	**92**
2[b]	UiO-67-CoH	65	0
3	No catalyst	0	0
4	UiO-67	14	13
5	UiO-67-CoCl	31	28
6	$CoCl_2$	10	8
7	Co@UiO-67	22	4
8	Co nanoparticles	18	11
9	$Co(OH)_2$	0	0
10	UiO-66-CoH	72	48
11[e]	UiO-67-CoH	62	29
12[f]	UiO-67-CoH	51	20

[a]Reaction conditions: 1.3 mmol of *p*-nitrotoluene**,** 0.012 g of UiO-67-CoH (0.75 mol% of Co), 10 bar CO_2 and 3 mL of solvent. [b]Nitrogen (10 bar) was used instead of CO_2. [c]Conversion of *p*-nitrotoluene was determined by GC-MS using area-percentage method. [d]Yield of *N*-*p*-tolylformamide was determined by GC using mesitylene as an internal standard. [e]1:1 mixture (5 bar CO_2 + 5 bar N_2) was used instead of CO_2. [f]1:1 mixture (2 bar CO_2 + 8 bar N_2) was used instead of CO_2.

3.3. Blank reaction of UiO-67-CoH with *p*-nitrotoluene without CO_2.

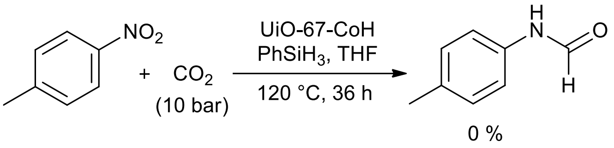

UiO-67-CoH (0.75 mol% of Co) in 3mL of THF was transferred into a glass liner. To this, *p*-nitrotoluene (1.3 mmol) and phenylsilane (2.5 equiv.) were added. The glass liner was then placed inside a high-pressure Parr reactor and subsequently sealed. The reactor was then taken out of the glovebox and purged 3 times with CO_2. It was then pressurized to 10 bar of CO_2 and heated at 120 °C for 36 h without any mechanical stirring. After the completion of the reaction, the reactor was cooled to room temperature, and the pressure was released gradually. The MOF was then separated from the reaction mixture by centrifugation, and the crude products were analyzed using GC-MS. The absence of *N*-*p*-tolylformamide confirmed that CO_2 was solely responsible for the *N*-formylation reaction with UiO-67-CoH MOF.

3.4. Test for "heterogeneity" of UiO-67-CoH in the *N*-formylation of *p*-nitrotoluene.

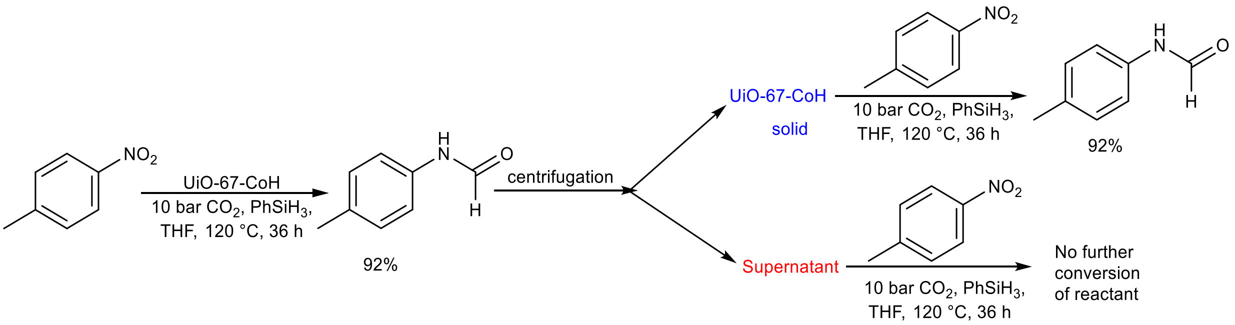

Figure S6. Hot filtration test of UiO-67-CoH for *N*-formylation of *p*-nitrotoluene.

In a glovebox, UiO-67-CoH (0.75 mol% of Co) in 3 mL of THF was transferred into a glass liner. To this mixture, *p*-nitrotoluene (1.3 mmol) and phenylsilane (2.5 equiv.) were added. The glass liner was then placed inside a high-pressure Parr reactor and subsequently sealed. The reactor was then taken out of the glovebox and purged 2-3 times with CO_2. It was then pressurized to 10 bar of CO_2 and heated at 120 °C for 36 h without any mechanical stirring. After the completion of the reaction, the pressure of the reactor was released. The solid MOF was removed from suspension to separate the solid and the supernatant, inside the glove box and washed with THF multiple times. The conversion analyzed by taking aliquots from the organic extract gave 92% of *N*-*p*-tolylformamide.

Two reactions were set up separately in two different Parr reactors, one with the solid MOF and the other one with the supernatant recovered from the previous reaction. The extracted solid and the supernatant were added to two separate liners, and to both the liners, *p*-nitrotoluene (1.3 mmol), phenylsilane (2.5 equiv.), and 3 mL of THF were added. Then both the liners were fitted into two separate Parr reactors and sealed. The sealed Parr reactors were then taken out from the glovebox and purged with CO_2 3 times. The reactors were pressurized to 10 bar of CO_2 and heated at 120 °C for 36 h without any mechanical stirring. After the completion of the reaction, the reactor was cooled to room temperature, and the pressure was released gradually. GC-MS analysis showed that the reaction with the solid MOF gave 90% yield of the desired product, while the reaction with the supernatant gave 0% conversion. This experiment excludes the potential of any leached Co-species responsible for catalysis and confirms that solid UiO-67-CoH was the actual catalyst for the formylation of *p*-nitrotoluene.

3.5. Hg Test.[4]

The catalytic activity of UiO-67-CoH in the *N*-formylation reaction was examined in the presence of a small amount of Hg^0. This was done to investigate whether any leached Co nanoparticles formed during the reaction participated in the catalytic reaction. The results showed that the rate of *N*-formylation reaction remained unchanged upon addition of Hg^0. This indicated that any potential leached Co-nanoparticles were not responsible for carrying out the catalytic reaction. These findings confirm that UiO-67-CoH acts as the actual catalyst in this reaction. Hence, it is concluded that UiO-67-CoH is the true catalyst for the *N*-formylation reaction. The experimental procedure of the reaction is as follows:

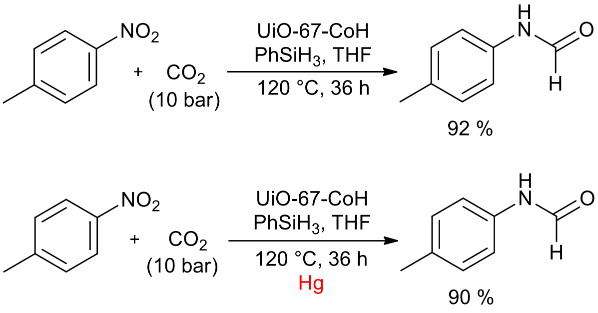

Figure S7. Hg test in the *N*-formylation of *p*-nitrotoluene catalyzed by UiO-67-CoH.

In a glovebox, UiO-67-CoH (0.75 mol% of Co) in 3 mL of THF was transferred into two separate glass liners. Each of the glass liners was charged with *p*-nitrotoluene (1.3 mmol) and phenylsilane (2.5 equiv.). To one of the liners, a drop of mercury was then added. Both the liners were placed inside a high-pressure Parr reactor and subsequently sealed. The sealed Parr reactors were then taken out of the glovebox and purged with CO_2 3 times. The reactors were pressurized to 10 bar of CO_2 and heated at 120 °C for 36 h without any mechanical stirring. After the completion of the reaction, the reactors were cooled to room temperature, and the pressure was released gradually. The MOF was then separated from the reaction mixtures by centrifugation, and the crude products were analyzed using GC-MS, which indicated almost similar results for both reactions. Hence, it can be concluded that leached Co particles did not participate in the catalytic activity, and that UiO-67-CoH acted as the actual catalyst.

3.6. Recycling of UiO-67-CoH for the formylation of *p*-nitrotoluene.

The recycle and reuse experiment was conducted to check the stability of UiO-67-CoH MOF-catalyst (Table S4). The detailed procedure of the recycling experiment is given below.

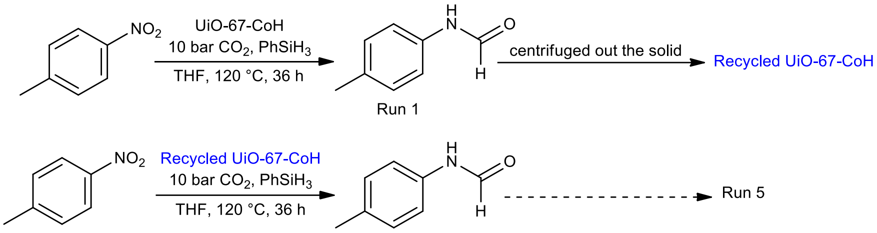

Figure S8. Recycle and reuse of UiO-67-CoH for the formylation of *p*-nitrotoluene.

Initially, in a glovebox, UiO-67-CoH (0.012g, 0.75 mol% of Co) in 3 mL of THF was transferred into a glass liner. To this mixture, *p*-nitrotoluene (1.3 mmol) and phenylsilane (2.5 equiv.) were added. The glass liner was then placed inside a high-pressure Parr reactor and subsequently sealed. The reactor was then taken out of the glovebox and purged 3 times with CO_2. It was then pressurized to 10 bar of CO_2 and heated at 120 °C for 36 h without any mechanical stirring. After the completion of the reaction, the reactor was cooled to room temperature, and the pressure was released gradually. The Paar reactor was then taken inside the glovebox, the solid MOF was centrifuged out from the suspension and washed with THF several times. The formylated product was analysed by GC-MS. The collected solid MOF was then reused for further reactions.

Inside the glovebox, the recovered MOF-catalyst was again added to the glass liner. 3 ml THF and *p*-nitrotoluene (1.3 mmol) were added to the glass tube and sealed in a Parr reactor. The Parr reactor was taken out from the glove box and was purged with the CO_2 gas for 2-3 times and then pressurized to 10 bar of CO_2. The reactor was heated at 120 °C for 36 h without any mechanical stirring. After the reaction, the solution was analyzed in the same way as mentioned previously in run 1. The recycling and reuse experiments were performed up to 4 times in total.

Table S4. %GC Yield of *N*-*p*-tolylformamide, the leaching of Co and Zr at various runs of the recycling of UiO-67-CoH in the *N*-formylation of *p*-nitrotoluene.

No. of Run	Time	%GC yield of *N*-*p*-tolylformamide	% Leaching (Co, Zr)
Run-1	36 h	92	0.05, 0.042
Run-2	36 h	89	
Run-3	36 h	88	0.09, 0.074
Run-4	36 h	82	
Run-5	36 h	78	

3.7. *N*-Formylation of *p*-nitrotoluene using Co(0) and Co@UiO-67.

3.7.1. Co(0) catalyzed *N*-formylation of nitro substrates.

Initially, $CoCl_2\cdot6H_2O$ (0.0024 g, 0.0084 mmol) was introduced to a glass vial containing 2 mL of THF inside the glovebox. Then, $NaEt_3BH$ (12 μL, 1 M in toluene) was added, and the mixture was stirred gently for 1 h to form black coloured Co nanoparticles. The resultant black solid was thoroughly washed with THF and dried. Then, a small amount of Co nanoparticles (0.25 mg, 0.0040 mmol Co) in 3 mL of THF was transferred into a glass liner, followed by the addition of *p*-nitrotoluene (1.3 mmol) and phenylsilane (2.5 equiv.) inside the glovebox and sealed in a Parr reactor. The Parr reactor was taken out of the glove box and was purged with the CO_2 gas for 2-3 times and then pressurized to 10 bar of CO_2. The reactor was heated at 120 °C for 36 h without any mechanical stirring. After the completion of the reaction, the reactor was cooled to room temperature, and the pressure was released gradually. The MOF was then separated from the reaction mixture by centrifugation, and the crude products were analyzed using GC-MS, which suggested that a negligible amount of the formylated product was formed from Co nanoparticles.

3.7.2. Co@UiO-67 catalyzed *N*-formylation.

$CoCl_2\cdot6H_2O$ (0.014 g, 0.058 mmol) was dissolved in 2 mL of ethyl acetate in a 25 mL round-bottom flask, and UiO-67 MOF (0.075 mg) was added to it. The mixture was heated at 50 °C for 48 h. Upon cooling to room temperature, the mixture was centrifuged out to isolate the MOF, which was washed and dried to afford UiO-67-CoCl. Then, $NaBH_4$ (0.015 g) was dissolved in 8 mL of deionized water, added to UiO-67-CoCl (0.070 mg) and stirred for 30 minutes. The solid product was collected by filtration, washed with deionized water, and dried to yield black Co@UiO-67 powder. The Co@UiO-67 sample was then activated at 150 °C for 12 h under high vacuum. For the catalytic reaction, inside a glovebox, 6 mg of Co@UiO-67 (0.002 mmol Co) dissolved in 3 mL of THF was added to *p*-nitrotoluene (1.3 mmol) and phenylsilane (2.5 equiv.) in a glass liner and sealed in a Parr reactor. The Parr reactor was taken out of the glove box and was purged with the CO_2 gas for 2-3 times and then pressurized to 10 bar CO_2. The reactor was heated at 120 °C for 36 h without any mechanical stirring. After the completion of the reaction, the reactor was cooled to room temperature, and the pressure was released gradually. GC-MS analysis of the crude products was performed, which revealed only 4% yield of the formylated product.

4. Determination of the rate law for UiO-67-CoH catalyzed *N*-formylation of *p*-nitrotoluene.

The kinetic analysis for the *N*-formylation of *p*-nitrotoluene was performed using the initial rate method, with conversions restricted to ≤10%. All reactions were carried out in 3 mL THF in a Parr reactor at 120 °C. For each experiment, a glass liner was charged under an N_2 atmosphere with UiO-67-CoH MOF catalyst, *p*-nitrotoluene, phenylsilane and THF. The liner was then placed inside the Parr reactor, sealed, pressurized with CO_2 to the desired pressure, and heated at 120 °C for 120 minutes. Product formation was quantified by GC-FID using mesitylene as an internal standard. Initial rates were obtained by monitoring the consumption of *p*-nitrotoluene during the first 120 minutes of reaction. Plots of *p*-nitrotolune concentration versus time were fitted by linear regression, and the slope (d[*p*-nitrotoluene]/dt) was taken as the initial rate for each experiment. All rates are reported in units of $mM \cdot min^{-1}$. The kinetic dependence of the reaction was examined by measuring the yield of *N*-*p*-tolyformamide across a range of *p*-nitrotoluene (0.7-4.46 mM) concentrations. Furthermore, the influence of catalyst concentration, CO_2 pressure and $PhSiH_3$ concentration on the *N*-*p*-tolyformamide yield was evaluated through reactions conducted with cobalt concentrations of (2.0×10^{-4} - 8.0×10^{-4} mM), CO_2 pressure (5-20 bar) and (2.5×10^{-1} - 5.0×10^{-1} mM) concentrations of $PhSiH_3$.

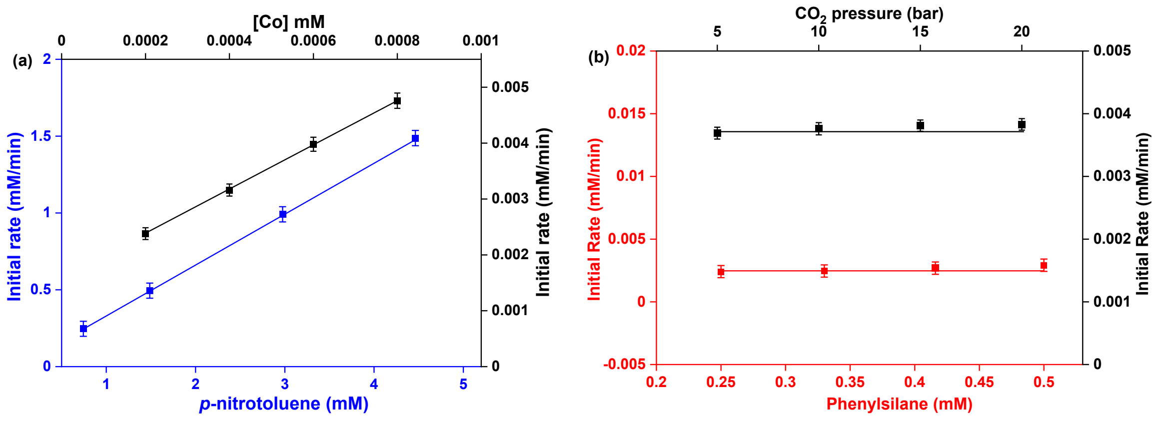

Figure S9. (a) Kinetic plots of initial rates (d[*p*-nitrotoluene]/dt) for the *N*-formylation of *p*-nitrotoluene versus initial concentrations of cobalt and *p*-nitrotoluene. (b) Kinetic plots of initial rates (d[*p*-nitrotoluene]/dt) for the *N*-formylation of *p*-nitrotoluene versus initial concentrations of $PhSiH_3$ and initial P_{CO2}.

5. EXAFS analysis.

Extended X-ray Absorption Fine Structure (EXAFS) measurements were conducted at the Energy-Scanning EXAFS beamline (BL-9) at the Indus-2 Synchrotron Source, located at the Raja Ramanna Centre for Advanced Technology (RRCAT) in Indore, India.[5] All measurements were conducted at room temperature. The beamline functions within an energy window of 4 keV to 25 keV. The beamline optical setup comprises of a Rh/Pt-coated collimaitng meridional cylindrical mirror, followed by the monochromatization of the beam by a Si(111) double crystal monochromator (DCM). The second crystal in the DCM, having a sagittal cylindrical geometry, enables horizontal beam focusing, while a Rh/Pt-coated bendable post-mirror, positioned downstream, provides vertical focusing at the sample position. X-ray absorption data were collected in transmission mode using two ionization chambers, each 300 mm in length. The first chamber measures the incident flux intensity, and the second one measures the transmitted flux. Metal foils were used for energy calibration. The gas mixture and pressure were optimized to achieve 10-20% absorption in the first ionization chamber and 70-90% absorption in the second, ensuring a high signal-to-noise ratio. For X-ray absorption measurements, powdered samples were homogeneously mixed with cellulose in an appropriate ratio and pressed into 15 mm pellets under 2 tons of pressure. The sample quantity was adjusted to obtain an optimal edge jump for the element under investigation. Spectra were recorded at the Co K-edge in transmission mode and calibrated against a reference metallic Co foil (7709 eV). Data reduction and analysis were performed using the Demeter software package.[6]

5.1 XANES analysis.

The oxidation state of the Co species within UiO-67-CoCl and UiO-67-CoH was determined by comparing its pre-edge and K-edge energy positions to that of $CoCl_2$. The pre-edge positions of UiO-67-CoCl (7709.10 eV) and UiO-67-CoH (7709.15 eV) closely matched to that of $CoCl_2$ (7709.4 eV). These results confirm the existence of Co in +2 oxidation state in UiO-67-CoCl and UiO-CoH.

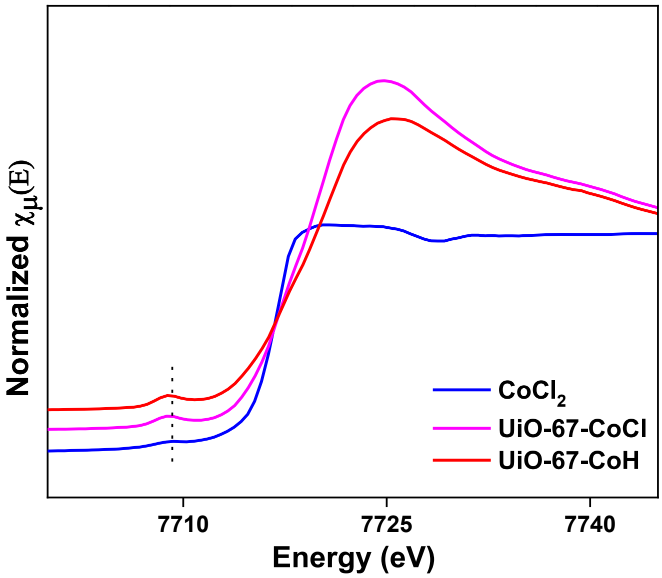

Figure S10. μ(E) XAS spectra of $CoCl_2$ (blue), UiO-67-CoH (magenta) and UiO-67-CoH (red).

5.2 EXAFS fitting using DFT optimized structures.

The spectra were calibrated using reference spectra and aligned to the first peak in the smoothed first derivative of the absorption spectrum. Background noise was eliminated, and the data were processed to achieve a normalized unit edge step. The fitting parameters for the Co-*K*-edge of UiO-67-CoH are detailed in Table S6 respectively.

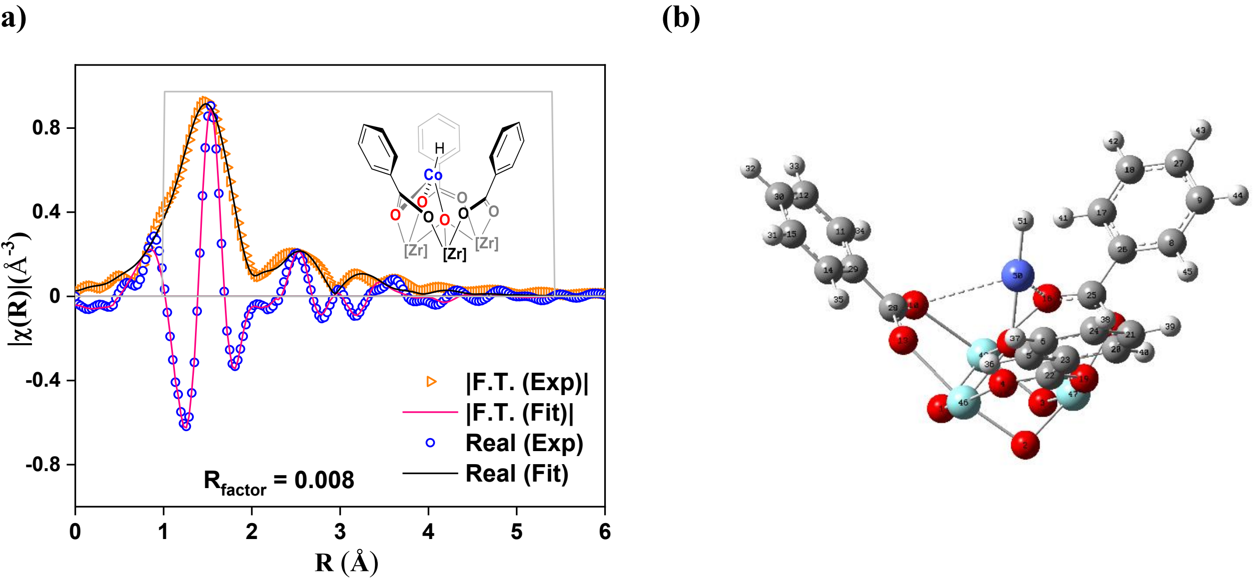

Figure S11. (a) EXAFS spectrum (hollow orange triangle and circle) and fits (pink and black solid lines) of UiO-67-CoH in the R space from 1.0-5.4 Å. (b) DFT optimized structure of UiO-67-CoH.

Table S5. Summary of EXAFS fitting parameters of UiO-67-CoH.

Sample	**UiO-67-CoH**
Fitting range	*k* 2.81-10.62 Å^{-1} R 1.0-5.4 Å
Independent points	22
R-factor	0.008
S_o^2	1.0
Variables	14
Reduced chi-square	63.1
ΔE_0 (eV)	-3.61±2.68
R(Co-O6)	1.94±0.52
R(Co-O7)	1.95±0.29
R(Co-C25)	2.08±0.08
R(Co-O22)	2.98±0.06
R(Co-Zr1)	3.07±0.15
R(Co-C26)	3.53±0.12
R(Co-O10)	3.33±0.06
R(Co-C28)	3.34±0.06
R(Co-C8)	3.95±0.12
R(Co-Zr2)	3.62±0.08
R(Co-C23)	4.43±0.12
R(Co-H)	1.44±0.11
σ^2 (Co-O)	0.008±0.002
σ^2 (Co-C)	0.006±0.005
σ^2 (Co-Zr)	0.015±0.007
σ^2 (Co-H)	0.004±0.018

6. DFT calculations.

All quantum chemical calculations were performed using the density functional theory (DFT) functional B3LYP-GD3BJ/def2svp implemented in the Gaussian 16 program.[7–11] Geometry optimizations of the electronic structures were optimized at the unrestricted level, and dispersion interactions were included via the Becke-Johnson (BJ) damping scheme (GD3BJ).[12] All computations were conducted in solution at 393.15 K using the polarizable continuum model (PCM) with the integral equation formalism variant (IEFPCM), as the default SCRF method by using tetrahydrofuran (THF) as the solvent. After geometry optimization, frequency calculations were performed at the same theoretical level to confirm the identity of each stationary step. Stable intermediates showed no imaginary frequencies, while transition states exhibited one imaginary mode associated with the specific bond-forming or bond-cleavage event occurring in that step of the reaction pathway. The DFT results indicate that the quatret spin state (S = 3/2) is the most stable configuration for Co(II) in all cases, as shown in Tables S6 and S7.

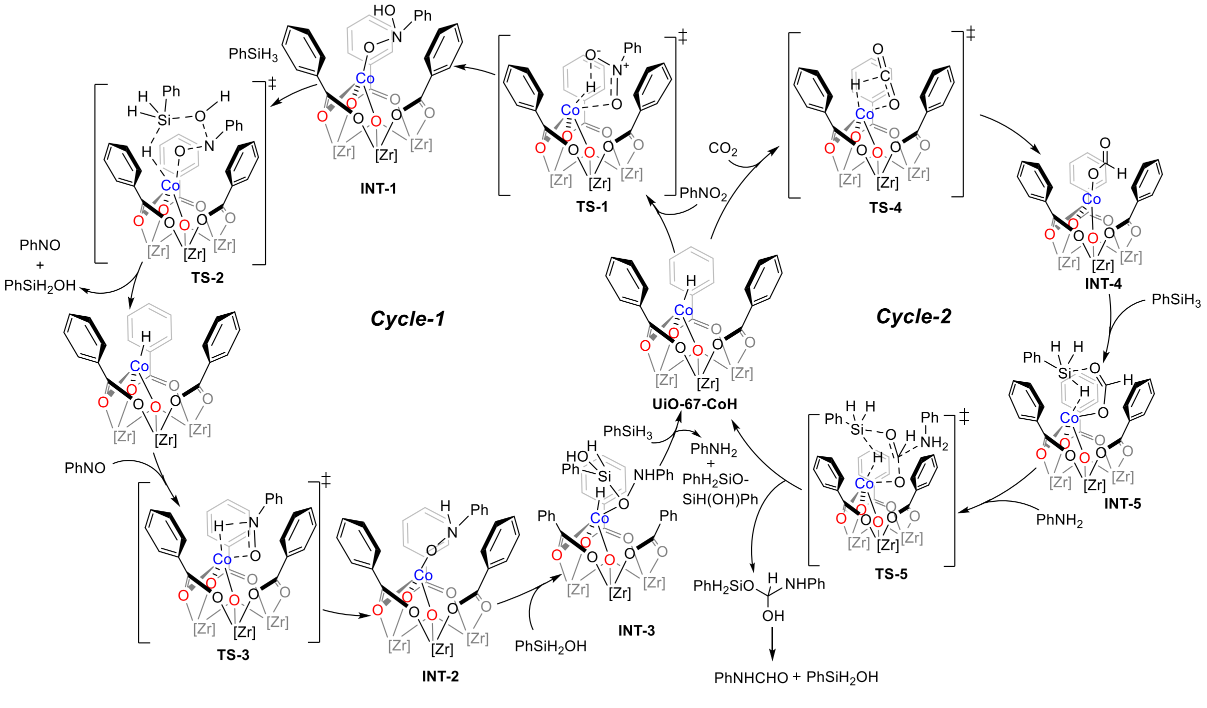

Figure S12. Proposed catalytic cycle of UiO-67-CoH catalyzed *N*-formylation reaction.

Table S6. Relative energies of the structures in the most stable spin state. All the structures are being geometry optimized for the catalytic cycle.

Structure	**O.S.**	**Quatret (S = 3/2)**
UiO-67-CoH	Co(II)	0
TS-1	Co(II)	25.719035
INT-1	Co(II)	-14.45007
TS-2	Co(II)	-8.6333675
UiO-67-CoH	Co(II)	-33.863665
TS-3	Co(II)	-22.455705
INT-2	Co(II)	-72.18007
INT-3	Co(II)	-68.0391975
UiO-67-CoH	Co(II)	-144.065215

Table S7. Relative energies of the structures in the most stable spin state. All the structures are being geometry optimized for the catalytic cycle.

Structure	**O.S.**	**Quatret (S = 3/2)**
UiO-67-CoH	Co(II)	0
TS-4	Co(II)	11.91748
INT-4	Co(II)	-9.56623775
INT-5	Co(II)	-17.696755
TS-5	Co(II)	-12.42199
UiO-67-CoH	Co(II)	-20.1805625

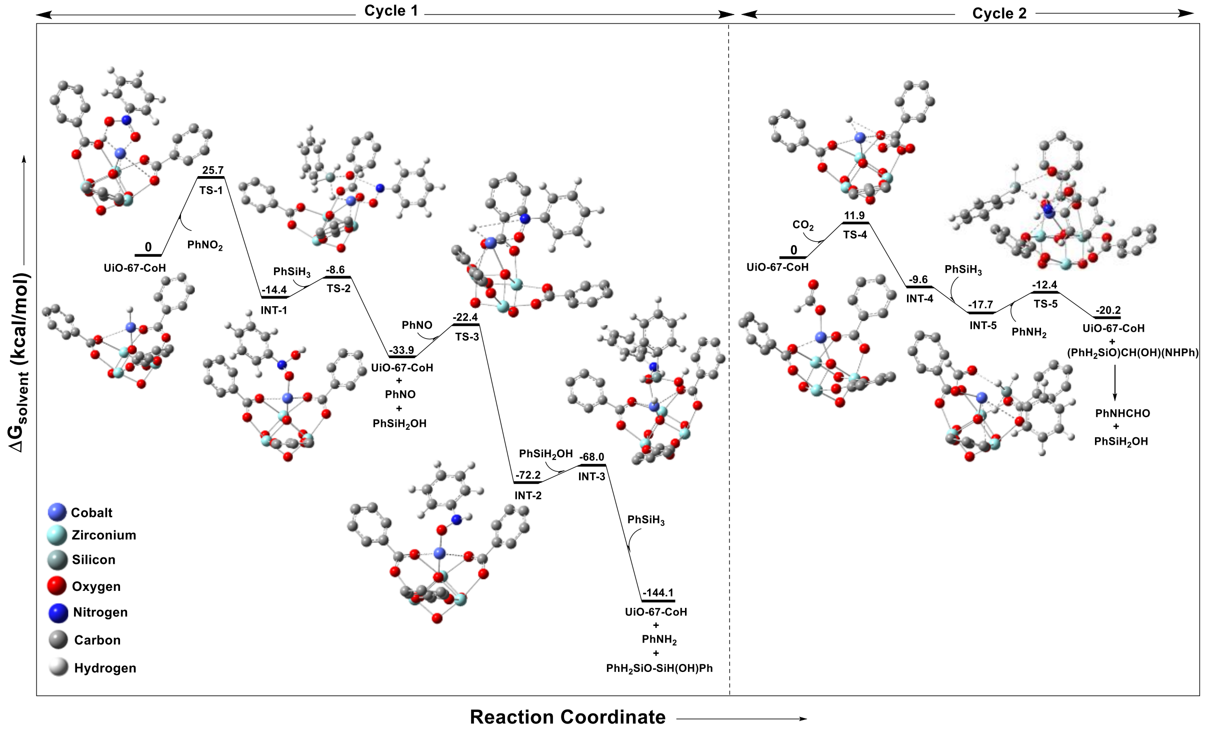

Figure S13. DFT-calculated free energy diagram for UiO-67-CoH catalyzed *N*-formylation reaction of nitro substrates at 393 K.

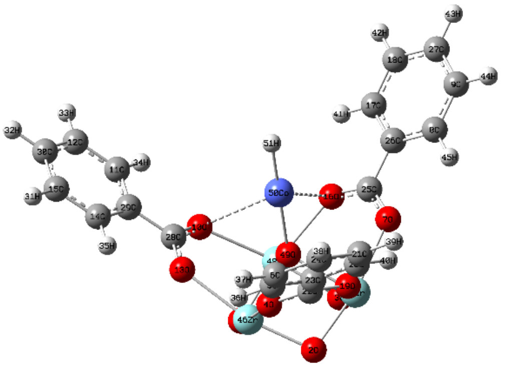

UiO-67-CoH

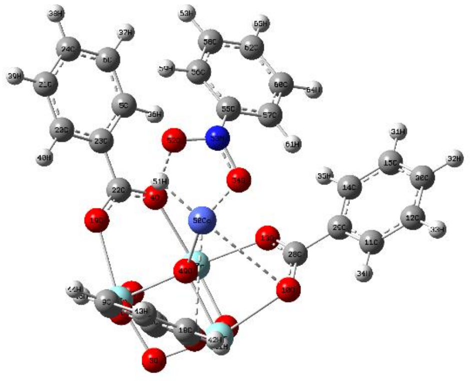

TS-1

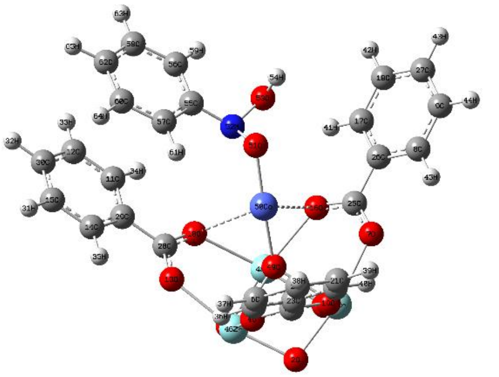

INT-1

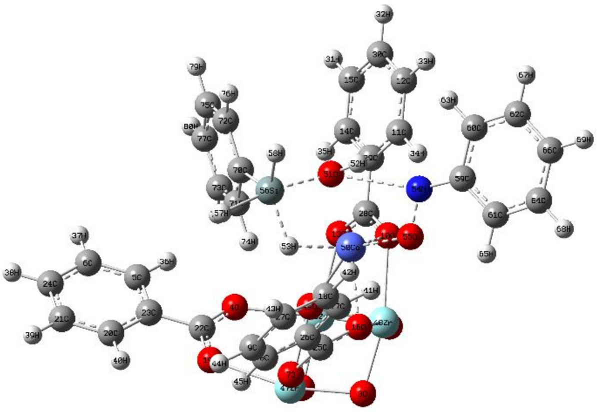

TS-2

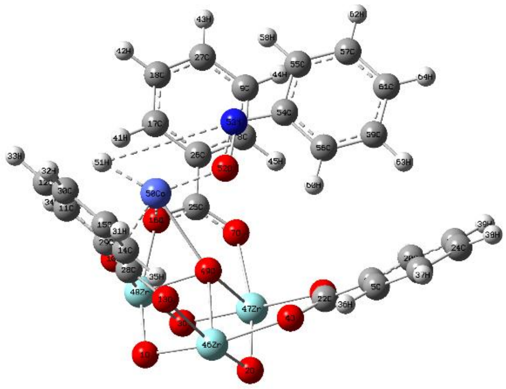

TS-3

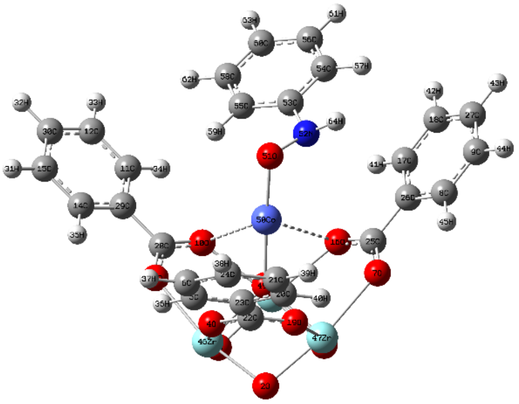

INT-2

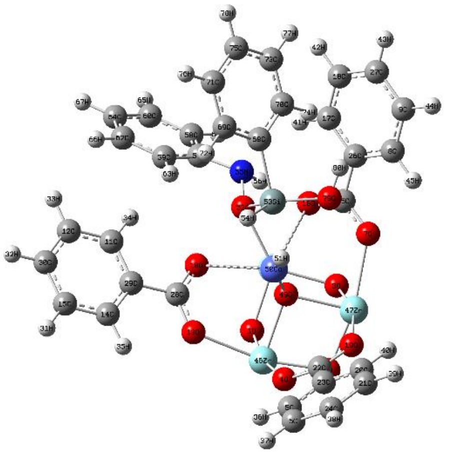

INT-3

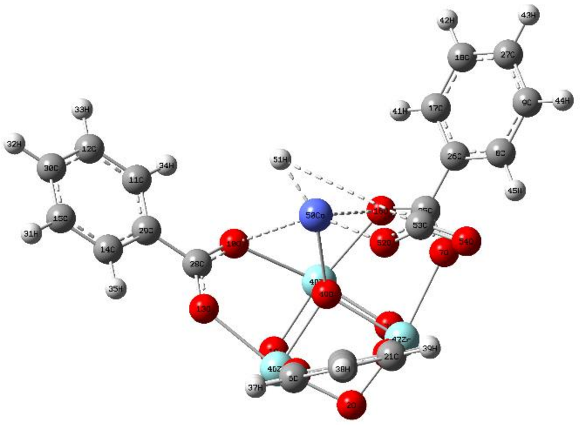

TS-4

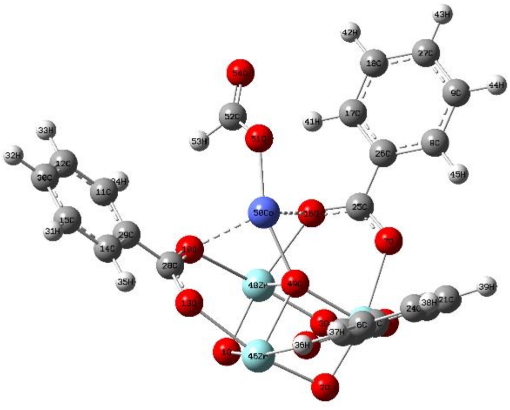

INT-4

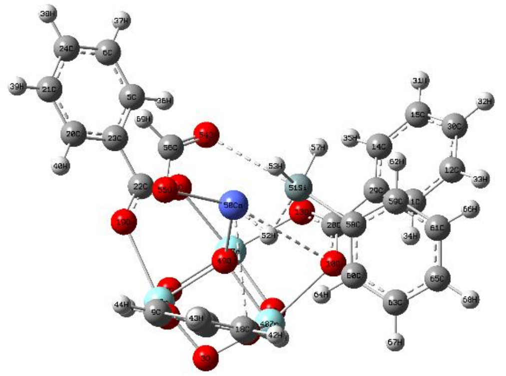

INT-5

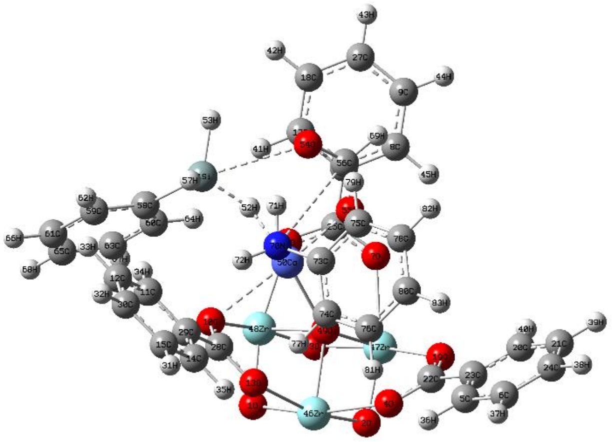

TS-5

Figure S14. DFT-optimized structures of different intermediates and transition states of the catalytic cycle in UiO-67-CoH catalysed *N*-formylation reaction of nitro substrates.

6.1. Cartesian Coordinates of Optimized Structures

Cartesian coordinates of UiO-67-CoH

Coordinates (Angstroms)

Atom No.	Atoms	X	Y	Z
1	O	49.515962	33.903564	47.564920
2	O	47.382028	31.936296	47.505497
3	O	47.520934	33.865141	49.605120
4	O	46.457830	32.610732	44.881943
5	C	44.646135	32.084006	42.816299
6	C	43.710048	31.832707	41.810162
7	O	44.951276	34.995435	49.351309
8	C	43.043038	36.913563	50.080253
9	C	42.119007	37.904328	50.421102
10	O	49.159162	36.530451	46.550771
11	C	49.902754	38.475899	44.672023
12	C	50.274012	39.412362	43.704249
13	O	48.999750	34.953012	44.953336
14	C	49.760135	36.764455	42.962378
15	C	50.132169	37.700164	41.994012
16	O	46.603334	36.521488	49.394486
17	C	44.823272	38.556928	50.126622
18	C	43.899921	39.548285	50.467483
19	O	44.824281	32.543561	46.428606
20	C	42.877510	32.045237	44.472430
21	C	41.940727	31.794888	43.466888
22	C	45.247061	32.464161	45.243395
23	C	44.238225	32.191182	44.156084
24	C	42.355415	31.687269	42.133630
25	C	45.396521	36.166304	49.537645
26	C	44.403148	37.230955	49.930586
27	C	42.545739	39.223837	50.615343
28	C	49.241664	36.134965	45.356335
29	C	49.643459	37.143852	44.309742
30	C	50.390296	39.026003	42.363229
31	H	50.221459	37.396285	40.947856
32	H	50.681734	39.758363	41.605803
33	H	50.473797	40.447002	43.994659
34	H	49.807963	38.762980	45.720594
35	H	49.555133	35.728274	42.688482
36	H	45.704624	32.200722	42.578185
37	H	44.036123	31.749957	40.770172
38	H	41.622715	31.490482	41.346603
39	H	40.883692	31.683034	43.721660
40	H	42.568542	32.131964	45.515457
41	H	45.880677	38.796826	50.003894
42	H	44.235201	40.577859	50.616824
43	H	41.822696	39.999645	50.880539
44	H	41.062252	37.648960	50.534195
45	H	42.723429	35.882337	49.921658
46	Zr	48.257344	33.168904	46.189154
47	Zr	46.084256	33.179326	48.390372
48	Zr	48.356893	35.274456	48.453476
49	O	46.901572	34.614487	47.047243
50	Co	46.261354	36.373527	46.671307
51	H	45.211669	36.948948	45.835453

Cartesian coordinates of TS-1

Coordinates (Angstroms)

Atom No.	Atoms	X	Y	Z
1	O	49.504477	33.995353	47.623615
2	O	47.370544	32.028084	47.564191
3	O	47.509449	33.956929	49.663814
4	O	46.446345	32.702520	44.940637
5	C	44.634650	32.175794	42.874993
6	C	43.698563	31.924495	41.868856
7	O	44.939791	35.087224	49.410003
8	C	43.031553	37.005352	50.138948
9	C	42.107522	37.996117	50.479796
10	O	49.147677	36.622239	46.609465
11	C	49.891269	38.567687	44.730717
12	C	50.262527	39.504150	43.762944

13	O	48.988265	35.044801	45.012031
14	C	49.748651	36.856244	43.021072
15	C	50.120684	37.791953	42.052707
16	O	46.591850	36.613276	49.453180
17	C	44.811788	38.648717	50.185317
18	C	43.888437	39.640074	50.526178
19	O	44.812797	32.635350	46.487301
20	C	42.866025	32.137025	44.531124
21	C	41.929243	31.886676	43.525583
22	C	45.235576	32.555950	45.302089
23	C	44.226741	32.282971	44.214778
24	C	42.343930	31.779057	42.192324
25	C	45.385037	36.258092	49.596339
26	C	44.391663	37.322744	49.989281
27	C	42.534255	39.315626	50.674037
28	C	49.230179	36.226753	45.415030
29	C	49.631974	37.235641	44.368437
30	C	50.378811	39.117792	42.421923
31	H	50.209974	37.488073	41.006550
32	H	50.670249	39.850152	41.664497
33	H	50.462312	40.538791	44.053354
34	H	49.796478	38.854768	45.779288
35	H	49.543648	35.820062	42.747176
36	H	45.693139	32.292510	42.636879
37	H	44.024638	31.841746	40.828866
38	H	41.611231	31.582270	41.405297
39	H	40.872207	31.774822	43.780355
40	H	42.557057	32.223752	45.574152
41	H	45.869192	38.888614	50.062588
42	H	44.223717	40.669648	50.675518
43	H	41.811211	40.091433	50.939234
44	H	41.050767	37.740748	50.592889
45	H	42.711944	35.974125	49.980352
46	Zr	48.245859	33.260693	46.247848
47	Zr	46.072771	33.271115	48.449067
48	Zr	48.345408	35.366244	48.512170
49	O	46.890087	34.706276	47.105937
50	Co	46.249869	36.465315	46.730001
51	H	44.730335	36.631591	46.664653
52	O	44.093156	38.098992	46.553597
53	N	45.325253	38.992105	46.524001
54	O	46.537396	37.971249	46.663352
55	C	45.381915	40.455469	46.396497
56	C	44.630750	41.099540	45.412935
57	C	46.186527	41.200119	47.258844
58	C	44.684767	42.487895	45.291384
59	H	43.997101	40.512121	44.732736
60	C	46.239911	42.588991	47.138025
61	H	46.778490	40.692667	48.034215
62	C	45.489320	43.232935	46.154417
63	H	44.093203	42.995576	44.515749
64	H	46.874084	43.175891	47.818354
65	H	45.531705	44.327598	46.058425

Cartesian coordinates of INT-1

Coordinates (Angstroms)

Atom No.	Atoms	X	Y	Z
1	O	50.105788	35.041714	46.747842
2	O	48.612068	32.694709	47.576974
3	O	48.740457	35.001460	49.253470
4	O	46.941980	32.595798	45.254636
5	C	44.890776	31.276143	43.884384
6	C	43.840147	30.626907	43.231395
7	O	45.981398	35.477262	49.579700
8	C	43.870129	37.050787	50.538057
9	C	42.828630	37.869336	50.981774
10	O	48.720580	37.229196	45.561395
11	C	48.575595	38.888098	43.242275
12	C	48.445143	39.660492	42.085654
13	O	48.721851	35.390636	44.267739
14	C	48.480347	36.869040	41.905637
15	C	48.350675	37.640758	40.748344
16	O	47.099405	37.265669	48.836805
17	C	45.114938	39.010214	49.842979
18	C	44.073923	39.829476	50.286431
19	O	45.803703	32.502952	47.193932

20	C	43.645023	31.204252	45.961700
21	C	42.593638	30.555897	45.309337
22	C	45.935296	32.271635	45.961497
23	C	44.802865	31.569272	45.255240
24	C	42.689567	30.265153	43.942812
25	C	46.135636	36.728948	49.463150
26	C	45.022483	37.613926	49.965354
27	C	42.928518	39.260494	50.856733
28	C	48.734994	36.653963	44.412794
29	C	48.595143	37.485935	43.162299
30	C	48.333277	39.038182	40.836116
31	H	48.262721	37.152615	39.774311
32	H	48.232143	39.642347	39.930722
33	H	48.430574	40.751117	42.156783
34	H	48.663386	39.359531	44.222553
35	H	48.494405	35.779257	41.851868
36	H	45.792528	31.564785	43.341938
37	H	43.917095	30.401817	42.164547
38	H	41.867356	29.756999	43.432190
39	H	41.695967	30.275666	45.866474
40	H	43.583753	31.437433	47.026012
41	H	46.011098	39.440155	49.392684
42	H	44.153492	40.914990	50.186104
43	H	42.113051	39.901205	51.202423
44	H	41.934819	37.422766	51.424955
45	H	43.803423	35.965130	50.625402
46	Zr	48.791286	33.785037	45.904620
47	Zr	47.285915	33.787143	48.606669
48	Zr	48.876380	36.286677	47.723448
49	O	47.351707	35.052993	46.895475
50	Co	46.113019	36.428769	46.237468
51	O	44.911150	37.763651	45.599019
52	N	45.830400	38.818529	45.560192
53	O	45.689791	39.602555	46.777160
54	H	44.706533	39.737518	46.850990
55	C	45.550359	39.675767	44.452828
56	C	46.078024	40.971536	44.438879
57	C	44.786776	39.218726	43.367486
58	C	45.840465	41.808469	43.348153
59	H	46.666530	41.301078	45.294077
60	C	44.562495	40.058324	42.276624
61	H	44.408407	38.200095	43.400055
62	C	45.086476	41.357657	42.258930
63	H	46.262289	42.816362	43.342735
64	H	43.966652	39.697694	41.434536
65	H	44.909945	42.012212	41.402987

Cartesian coordinates of TS-2

Coordinates (Angstroms)

Atom No.	Atoms	X	Y	Z
1	O	50.210625	35.371821	48.578144
2	O	48.076670	33.404528	48.518732
3	O	48.215511	35.333431	50.618380
4	O	47.152457	34.078948	45.895182
5	C	45.340768	33.552235	43.829525
6	C	44.404680	33.300936	42.823388
7	O	45.645893	36.463662	50.364523
8	C	43.737663	38.381791	51.093469
9	C	42.813639	39.372559	51.434330
10	O	49.836304	37.997793	47.564924
11	C	50.597387	39.944129	45.685250
12	C	50.968646	40.880592	44.717476
13	O	49.694418	36.421222	45.966552
14	C	50.454769	38.232685	43.975604
15	C	50.826803	39.168394	43.007239
16	O	47.298235	37.989359	50.407628
17	C	45.517905	40.025159	51.139850
18	C	44.594554	41.016516	51.480711
19	O	45.518911	34.011793	47.441834
20	C	43.572142	33.513466	45.485657
21	C	42.635359	33.263116	44.480115
22	C	45.941694	33.932390	46.256622
23	C	44.932858	33.659411	45.169310
24	C	43.050047	33.155498	43.146856
25	C	46.091041	37.634959	50.550979
26	C	45.097777	38.699190	50.943793

27	C	43.240372	40.692068	51.628571
28	C	49.936188	37.603263	46.369530
29	C	50.338103	38.612080	45.322971
30	C	51.084930	40.494233	43.376455
31	H	50.916092	38.864515	41.961081
32	H	51.376368	41.226594	42.619029
33	H	51.168430	41.915233	45.007886
34	H	50.502596	40.231210	46.733821
35	H	50.249766	37.196504	43.701708
36	H	46.399257	33.668951	43.591411
37	H	44.730756	33.218186	41.783397
38	H	42.317347	32.958710	42.359829
39	H	41.578324	33.151263	44.734887
40	H	43.263174	33.600193	46.528684
41	H	46.575310	40.265056	51.017121
42	H	44.929834	42.046090	51.630052
43	H	42.517328	41.467875	51.893767
44	H	41.756884	39.117190	51.547423
45	H	43.418061	37.350567	50.934886
46	Zr	48.952043	34.637127	47.202495
47	Zr	46.779030	34.647545	49.403674
48	Zr	49.051448	36.742385	49.466655
49	O	47.610976	36.283054	48.077659
50	Co	47.845313	38.921799	48.412703
51	O	47.730927	40.115070	46.749335
52	H	48.079994	40.917454	47.197263
53	H	46.088385	38.939908	47.966195
54	N	48.971579	41.403564	48.838971
55	O	48.639248	40.349623	49.558980
56	Si	45 .910647	39.811983	46.648248
57	H	44.390542	39.454093	46.801161
58	H	45.634505	41.298284	46.584887
59	C	49.651420	42.379142	49.532801
60	C	50.049714	43.532652	48.808219
61	C	49.974581	42.303795	50.913306
62	C	50.742575	44.561516	49.436082
63	H	49.796105	43.586688	47.746567
64	C	50.668867	43.343234	51.527815
65	H	49.663380	41.421556	51.472021
66	C	51.059976	44.478037	50.802057
67	H	51.041268	45.442113	48.860673
68	H	50.910213	43.273226	52.592686
69	H	51.603687	45.288238	51.293479
70	C	46.200840	38.856413	45.031099
71	C	46.527428	37.488429	45.058549
72	C	46.204542	39.500958	43.780350
73	C	46.859191	36.796738	43.890056
74	H	46.557776	36.958092	46.013277
75	C	46.520347	38.811339	42.604932
76	H	45.972722	40.568999	43.718542
77	C	46.854753	37.454077	42.656747
78	H	47.132360	35.743487	43.955016
79	H	46.517789	39.338411	41.646429
80	H	47.115819	36.914740	41.742075

Cartesian coordinates of TS-3

Coordinates (Angstroms)

Atom No.	Atoms	X	Y	Z
1	O	49.961123	35.080503	46.685418
2	O	48.467390	32.733461	47.514579
3	O	48.595795	35.040202	49.191068
4	O	46.797310	32.634531	45.192278
5	C	44.746103	31.314899	43.821991
6	C	43.695474	30.665663	43.169003
7	O	45.836762	35.516038	49.517322
8	C	43.725456	37.089543	50.475664
9	C	42.683957	37.908092	50.919382
10	O	48.576213	37.267879	45.498608
11	C	48.430922	38.926854	43.179882
12	C	48.300470	39.699248	42.023262
13	O	48.577066	35.429370	44.205324
14	C	48.335674	36.907796	41.843245
15	C	48.206001	37.679514	40.685952
16	O	46.954569	37.304373	48.774304
17	C	44.970265	39.048969	49.780587
18	C	43.929250	39.868232	50.224038

19	O	45.658999	32.541728	47.131554
20	C	43.500350	31.243008	45.899307
21	C	42.448965	30.594653	45.246945
22	C	45.790623	32.310391	45.899105
23	C	44.658192	31.608028	45.192848
24	C	42.544894	30.303909	43.880419
25	C	45.990991	36.767645	49.400750
26	C	44.877818	37.652684	49.902976
27	C	42.783844	39.299250	50.794340
28	C	48.590308	36.693000	44.350261
29	C	48.450518	37.524696	43.099905
30	C	48.188604	39.076938	40.773723
31	H	48.118048	37.191371	39.711919
32	H	48.087469	39.681103	39.868329
33	H	48.285900	40.789873	42.094391
34	H	48.518713	39.398287	44.160161
35	H	48.349731	35.818013	41.789475
36	H	45.647855	31.603541	43.279545
37	H	43.772422	30.440572	42.102154
38	H	41.722683	29.795754	43.369797
39	H	41.551294	30.314422	45.804082
40	H	43.439080	31.476189	46.963620
41	H	45.866425	39.478911	49.330291
42	H	44.008818	40.953746	50.123711
43	H	41.968378	39.939961	51.140030
44	H	41.790146	37.461522	51.362563
45	H	43.658749	36.003886	50.563009
46	Zr	48.646916	33.824091	45.842288
47	Zr	47.140983	33.825713	48.544129
48	Zr	48.731764	36.325263	47.660901
49	O	47.176257	35.237215	46.816356
50	Co	46.672291	37.637742	46.525856
51	H	46.861175	39.281796	46.645997
52	O	45.033615	36.549363	46.611657
53	N	43.939068	37.249263	46.785581
54	C	42.823245	36.484142	47.025130
55	C	41.611713	37.156388	47.330060
56	C	42.816127	35.060111	46.999136
57	C	40.453198	36.441196	47.611913
58	H	41.625969	38.248067	47.350225
59	C	41.646620	34.359391	47.279043
60	H	43.741020	34.539213	46.749576
61	C	40.456701	35.035815	47.592272
62	H	39.531488	36.979102	47.851913
63	H	41.655533	33.265254	47.246449
64	H	39.543939	34.477389	47.813774

Cartesian coordinates of INT-2

Coordinates (Angstroms)

Atom No.	Atoms	X	Y	Z
1	O	50.105775	35.041738	46.747795
2	O	48.612133	32.694754	47.577010
3	O	48.740260	35.001549	49.253527
4	O	46.941986	32.595757	45.254696
5	C	44.890776	31.276143	43.884384
6	C	43.840147	30.626907	43.231395
7	O	45.981398	35.477258	49.579710
8	C	43.870129	37.050787	50.538057
9	C	42.828630	37.869336	50.981774
10	O	48.720594	37.229993	45.560947
11	C	48.575595	38.888098	43.242275
12	C	48.445143	39.660492	42.085654
13	O	48.721525	35.390599	44.267697
14	C	48.480347	36.869040	41.905637
15	C	48.350675	37.640758	40.748344
16	O	47.099747	37.266064	48.837386
17	C	45.114938	39.010214	49.842979
18	C	44.073923	39.829476	50.286431
19	O	45.803709	32.502948	47.193930
20	C	43.645023	31.204252	45.961700
21	C	42.593638	30.555897	45.309337
22	C	45.935296	32.271635	45.961497
23	C	44.802865	31.569272	45.255240
24	C	42.689567	30.265153	43.942812
25	C	46.135538	36.728907	49.462963
26	C	45.022522	37.613936	49.965422

27	C	42.928518	39.260494	50.856733
28	C	48.735482	36.653830	44.412868
29	C	48.595186	37.485939	43.162297
30	C	48.333277	39.038182	40.836116
31	H	48.262721	37.152615	39.774311
32	H	48.232143	39.642347	39.930722
33	H	48.430574	40.751117	42.156783
34	H	48.663386	39.359531	44.222553
35	H	48.494405	35.779257	41.851868
36	H	45.792528	31.564785	43.341938
37	H	43.917095	30.401817	42.164547
38	H	41.867356	29.756999	43.432190
39	H	41.695967	30.275666	45.866474
40	H	43.583753	31.437433	47.026012
41	H	46.011098	39.440155	49.392684
42	H	44.153492	40.914990	50.186104
43	H	42.113051	39.901205	51.202423
44	H	41.934819	37.422766	51.424955
45	H	43.803423	35.965130	50.625402
46	Zr	48.791712	33.785530	45.904609
47	Zr	47.285731	33.787243	48.606736
48	Zr	48.876596	36.286364	47.723271
49	O	47.350883	35.051606	46.895437
50	Co	45.648651	35.771260	46.350267
51	O	43.942003	36.354218	45.923459
52	N	43.942689	37.534616	46.700962
53	C	44.182989	38.739088	46.063347
54	C	43.773929	39.951878	46.663578
55	C	44.915285	38.789620	44.859964
56	C	44.094970	41.170452	46.068753
57	H	43.205989	39.925280	47.598823
58	C	45.218179	40.018474	44.272435
59	H	45.236131	37.849686	44.403896
60	C	44.822476	41.219488	44.869331
61	H	43.763855	42.097499	46.550385
62	H	45.788627	40.028769	43.337800
63	H	45.065864	42.180486	44.404836
64	H	43.177187	37.542852	47.370968

Cartesian coordinates of INT-3

Coordinates (Angstroms)

Atom No.	Atoms	X	Y	Z
1	O	50.105775	35.041738	46.747795
2	O	48.612133	32.694754	47.577010
3	O	48.740260	35.001549	49.253527
4	O	46.941986	32.595757	45.254696
5	C	44.890776	31.276143	43.884384
6	C	43.840147	30.626907	43.231395
7	O	45.981398	35.477258	49.579710
8	C	43.870129	37.050787	50.538057
9	C	42.828630	37.869336	50.981774
10	O	48.720594	37.229993	45.560947
11	C	48.575595	38.888098	43.242275
12	C	48.445143	39.660492	42.085654
13	O	48.721525	35.390599	44.267697
14	C	48.480347	36.869040	41.905637
15	C	48.350675	37.640758	40.748344
16	O	47.099747	37.266064	48.837386
17	C	45.114938	39.010214	49.842979
18	C	44.073923	39.829476	50.286431
19	O	45.803709	32.502948	47.193930
20	C	43.645023	31.204252	45.961700
21	C	42.593638	30.555897	45.309337
22	C	45.935296	32.271635	45.961497
23	C	44.802865	31.569272	45.255240
24	C	42.689567	30.265153	43.942812
25	C	46.135538	36.728907	49.462963
26	C	45.022522	37.613936	49.965422
27	C	42.928518	39.260494	50.856733
28	C	48.735482	36.653830	44.412868
29	C	48.595186	37.485939	43.162297
30	C	48.333277	39.038182	40.836116
31	H	48.262721	37.152615	39.774311
32	H	48.232143	39.642347	39.930722
33	H	48.430574	40.751117	42.156783
34	H	48.663386	39.359531	44.222553

35	H	48.494405	35.779257	41.851868
36	H	45.792528	31.564785	43.341938
37	H	43.917095	30.401817	42.164547
38	H	41.867356	29.756999	43.432190
39	H	41.695967	30.275666	45.866474
40	H	43.583753	31.437433	47.026012
41	H	46.011098	39.440155	49.392684
42	H	44.153492	40.914990	50.186104
43	H	42.113051	39.901205	51.202423
44	H	41.934819	37.422766	51.424955
45	H	43.803423	35.965130	50.625402
46	Zr	48.791712	33.785530	45.904609
47	Zr	47.285731	33.787243	48.606736
48	Zr	48.876596	36.286364	47.723271
49	O	47.350883	35.051606	46.895437
50	Co	45.648651	35.771260	46.350267
51	O	43.942003	36.354218	45.923459
52	N	43.942689	37.534616	46.700962
53	C	44.182989	38.739088	46.063347
54	C	43.773929	39.951878	46.663578
55	C	44.915285	38.789620	44.859964
56	C	44.094970	41.170452	46.068753
57	H	43.205989	39.925280	47.598823
58	C	45.218179	40.018474	44.272435
59	H	45.236131	37.849686	44.403896
60	C	44.822476	41.219488	44.869331
61	H	43.763855	42.097499	46.550385
62	H	45.788627	40.028769	43.337800
63	H	45.065864	42.180486	44.404836
64	H	43.177187	37.542852	47.370968

Cartesian coordinates of TS-4

Coordinates (Angstroms)

Atom No.	Atoms	X	Y	Z
1	O	49.961123	35.080503	46.685418
2	O	48.467390	32.733461	47.514579
3	O	48.595795	35.040202	49.191068
4	O	46.797310	32.634531	45.192278
5	C	44.746103	31.314899	43.821991
6	C	43.695474	30.665663	43.169003
7	O	45.836762	35.516038	49.517322
8	C	43.725456	37.089543	50.475664
9	C	42.683957	37.908092	50.919382
10	O	48.576213	37.267879	45.498608
11	C	48.430922	38.926854	43.179882
12	C	48.300470	39.699248	42.023262
13	O	48.577066	35.429370	44.205324
14	C	48.335674	36.907796	41.843245
15	C	48.206001	37.679514	40.685952
16	O	46.954569	37.304373	48.774304
17	C	44.970265	39.048969	49.780587
18	C	43.929250	39.868232	50.224038
19	O	45.658999	32.541728	47.131554
20	C	43.500350	31.243008	45.899307
21	C	42.448965	30.594653	45.246945
22	C	45.790623	32.310391	45.899105
23	C	44.658192	31.608028	45.192848
24	C	42.544894	30.303909	43.880419
25	C	45.990991	36.767645	49.400750
26	C	44.877818	37.652684	49.902976
27	C	42.783844	39.299250	50.794340
28	C	48.590308	36.693000	44.350261
29	C	48.450518	37.524696	43.099905
30	C	48.188604	39.076938	40.773723
31	H	48.118048	37.191371	39.711919
32	H	48.087469	39.681103	39.868329
33	H	48.285900	40.789873	42.094391
34	H	48.518713	39.398287	44.160161
35	H	48.349731	35.818013	41.789475
36	H	45.647855	31.603541	43.279545
37	H	43.772422	30.440572	42.102154
38	H	41.722683	29.795754	43.369797
39	H	41.551294	30.314422	45.804082
40	H	43.439080	31.476189	46.963620
41	H	45.866425	39.478911	49.330291
42	H	44.008818	40.953746	50.123711

43	H	41.968378	39.939961	51.140030
44	H	41.790146	37.461522	51.362563
45	H	43.658749	36.003886	50.563009
46	Zr	48.646916	33.824091	45.842288
47	Zr	47.140983	33.825713	48.544129
48	Zr	48.731764	36.325263	47.660901
49	O	47.206809	35.091691	46.833967
50	Co	45.767616	36.798906	46.323054
51	H	45.934966	38.368953	46.067601
52	O	44.518250	35.307383	46.735683
53	C	43.346892	35.762402	46.565545
54	O	42.266145	35.364783	46.959651

Cartesian coordinates of INT-4

Coordinates (Angstroms)

Atom No.	Atoms	X	Y	Z
1	O	50.105792	35.041745	46.747807
2	O	48.612060	32.694703	47.576968
3	O	48.740465	35.001444	49.253457
4	O	46.941980	32.595772	45.254667
5	C	44.890772	31.276141	43.884381
6	C	43.840144	30.626905	43.231392
7	O	45.981432	35.477279	49.579711
8	C	43.870126	37.050784	50.538053
9	C	42.828627	37.869333	50.981770
10	O	48.720882	37.229121	45.560997
11	C	48.575592	38.888095	43.242272
12	C	48.445139	39.660490	42.085651
13	O	48.721735	35.390611	44.267713
14	C	48.480343	36.869038	41.905634
15	C	48.350671	37.640756	40.748341
16	O	47.099239	37.265614	48.836693
17	C	45.114935	39.010211	49.842975
18	C	44.073920	39.829473	50.286427
19	O	45.803668	32.502970	47.193943
20	C	43.645020	31.204250	45.961696
21	C	42.593635	30.555895	45.309334
22	C	45.935293	32.271633	45.961494
23	C	44.802861	31.569270	45.255237
24	C	42.689564	30.265151	43.942808
25	C	46.135661	36.728887	49.463139
26	C	45.022488	37.613925	49.965365
27	C	42.928515	39.260491	50.856729
28	C	48.734977	36.654241	44.412650
29	C	48.595188	37.485937	43.162294
30	C	48.333274	39.038179	40.836113
31	H	48.262718	37.152612	39.774308
32	H	48.232139	39.642344	39.930719
33	H	48.430570	40.751114	42.156780
34	H	48.663382	39.359528	44.222550
35	H	48.494401	35.779254	41.851864
36	H	45.792525	31.564783	43.341934
37	H	43.917092	30.401814	42.164544
38	H	41.867353	29.756996	43.432186
39	H	41.695964	30.275664	45.866471
40	H	43.583750	31.437431	47.026009
41	H	46.011095	39.440152	49.392680
42	H	44.153488	40.914987	50.186100
43	H	42.113048	39.901203	51.202419
44	H	41.934816	37.422763	51.424952
45	H	43.803419	35.965127	50.625398
46	Zr	48.791586	33.785332	45.904677
47	Zr	47.285652	33.786954	48.606518
48	Zr	48.876434	36.286504	47.723290
49	O	47.351479	35.052932	46.896356
50	Co	46.359185	36.580679	46.519541
51	O	44.698117	36.768761	45.799902
52	C	44.457157	38.148041	45.509345
53	H	45.210021	38.877506	45.723765
54	O	43.362725	38.506847	45.002345

Cartesian coordinates of INT-5

Coordinates (Angstroms)

Atom No. Atoms X Y Z

1	O	50.210577	35.371782	48.578137
2	O	48.076661	33.404522	48.518723
3	O	48.215540	35.333370	50.618331
4	O	47.152456	34.078957	45.895162
5	C	45.340761	33.552230	43.829519
6	C	44.404674	33.300931	42.823382
7	O	45.645897	36.463659	50.364524
8	C	43.737660	38.381788	51.093470
9	C	42.813632	39.372553	51.434322
10	O	49.836683	37.998052	47.564569
11	C	50.597380	39.944123	45.685243
12	C	50.968638	40.880586	44.717469
13	O	49.694363	36.421241	45.966557
14	C	50.454762	38.232680	43.975598
15	C	50.826795	39.168389	43.007232
16	O	47.297884	37.989771	50.408041
17	C	45.517898	40.025153	51.139843
18	C	44.594547	41.016510	51.480704
19	O	45.518912	34.011781	47.441825
20	C	43.572136	33.513461	45.485650
21	C	42.635353	33.263112	44.480108
22	C	45.941687	33.932385	46.256615
23	C	44.932851	33.659406	45.169304
24	C	43.050041	33.155493	43.146850
25	C	46.091170	37.634436	50.550824
26	C	45.097776	38.699178	50.943817
27	C	43.240365	40.692062	51.628564
28	C	49.936313	37.602904	46.369652
29	C	50.338093	38.612075	45.322964
30	C	51.084922	40.494228	43.376449
31	H	50.916085	38.864509	41.961075
32	H	51.376361	41.226588	42.619023
33	H	51.168423	41.915227	45.007879
34	H	50.502589	40.231205	46.733814
35	H	50.249759	37.196498	43.701702
36	H	46.399250	33.668946	43.591405
37	H	44.730749	33.218181	41.783391
38	H	42.317341	32.958706	42.359822
39	H	41.578318	33.151258	44.734880
40	H	43.263168	33.600188	46.528677
41	H	46.575303	40.265050	51.017114
42	H	44.929827	42.046084	51.630044
43	H	42.517322	41.467870	51.893760
44	H	41.756878	39.117184	51.547416
45	H	43.418055	37.350561	50.934878
46	Zr	48.951959	34.637117	47.202376
47	Zr	46.778883	34.647582	49.403627
48	Zr	49.051563	36.742756	49.466651
49	O	47.596093	36.082626	48.060228
50	Co	46.485930	37.352720	46.884096
51	Si	46.614393	39.674540	46.432325
52	H	47.220010	38.601172	47.494751
53	H	45.179587	40.071543	46.578844
54	O	45.150690	36.990700	45.343302
55	O	44.287807	37.093931	47.381522
56	C	44.166312	36.915319	46.145612
57	H	46.979516	39.640549	44.981958
58	C	47.681484	41.041691	47.192372
59	C	48.059790	42.176029	46.453716
60	C	48.146621	40.929160	48.514800
61	C	48.877691	43.163041	47.011540
62	H	47.730097	42.283461	45.416138
63	C	48.962912	41.913039	49.080699
64	H	47.874855	40.051450	49.107367
65	C	49.333796	43.032174	48.327502
66	H	49.167879	44.032513	46.415882
67	H	49.314655	41.805484	50.110515
68	H	49.978002	43.799676	48.764105
69	H	43.167192	36.676600	45.714296

Cartesian coordinates of TS-5

Coordinates (Angstroms)

Atom No.	Atoms	X	Y	Z
1	O	50.210602	35.371812	48.578128
2	O	48.076672	33.404528	48.518734
3	O	48.215508	35.333412	50.618355

4	O	47.152462	34.078960	45.895170
5	C	45.340768	33.552235	43.829525
6	C	44.404680	33.300936	42.823388
7	O	45.645907	36.463658	50.364557
8	C	43.737663	38.381791	51.093469
9	C	42.813639	39.372559	51.434330
10	O	49.836699	37.997808	47.564899
11	C	50.597387	39.944129	45.685250
12	C	50.968646	40.880592	44.717476
13	O	49.694389	36.421234	45.966555
14	C	50.454769	38.232685	43.975604
15	C	50.826803	39.168394	43.007239
16	O	47.298056	37.989562	50.407489
17	C	45.517905	40.025159	51.139850
18	C	44.594554	41.016516	51.480711
19	O	45.518922	34.011783	47.441830
20	C	43.572142	33.513466	45.485657
21	C	42.635359	33.263116	44.480115
22	C	45.941694	33.932390	46.256622
23	C	44.932858	33.659411	45.169310
24	C	43.050047	33.155498	43.146856
25	C	46.091121	37.634657	50.550899
26	C	45.097777	38.699189	50.943795
27	C	43.240372	40.692068	51.628571
28	C	49.936212	37.603302	46.369519
29	C	50.338114	38.612077	45.322972
30	C	51.084930	40.494233	43.376455
31	H	50.916092	38.864515	41.961081
32	H	51.376368	41.226594	42.619029
33	H	51.168430	41.915233	45.007886
34	H	50.502596	40.231210	46.733821
35	H	50.249766	37.196504	43.701708
36	H	46.399257	33.668951	43.591411
37	H	44.730756	33.218186	41.783397
38	H	42.317347	32.958710	42.359829
39	H	41.578324	33.151263	44.734887
40	H	43.263174	33.600193	46.528684
41	H	46.575310	40.265056	51.017121
42	H	44.929834	42.046090	51.630052
43	H	42.517328	41.467875	51.893767
44	H	41.756884	39.117190	51.547423
45	H	43.418061	37.350567	50.934886
46	Zr	48.952028	34.637148	47.202436
47	Zr	46.779000	34.647533	49.403643
48	Zr	49.051664	36.742533	49.466605
49	O	47.595810	36.082701	48.060543
50	Co	47.399727	38.239767	47.716812
51	Si	48.057617	41.123113	48.474213
52	H	47.487604	39.756913	48.697105
53	H	47.148267	42.120235	49.105681
54	O	45.311482	40.544698	47.309377
55	O	45.369960	38.391179	47.966326
56	C	44.815371	39.523052	47.822097
57	H	48.265602	41.457775	47.044268
58	C	49.717572	41.077285	49.367579
59	C	50.848614	41.766367	48.896539
60	C	49.855617	40.300980	50.536009
61	C	52.078942	41.672947	49.555710
62	H	50.776605	42.377551	47.992391
63	C	51.082532	40.205685	51.200279
64	H	48.992997	39.754768	50.928088
65	C	52.199570	40.889507	50.707259
66	H	52.947374	42.210130	49.166400
67	H	51.167686	39.599434	52.106312
68	H	53.160915	40.813480	51.221141
69	H	43.762622	39.581942	48.200219
70	N	47.238030	39.054107	45.735055
71	H	46.719923	39.883567	46.050019
72	H	48.146381	39.329119	45.356158
73	C	46.471668	38.335396	44.774038
74	C	47.043433	37.266059	44.069763
75	C	45.133116	38.679060	44.533043
76	C	46.294591	36.581033	43.113860
77	H	48.067777	36.970695	44.290003
78	C	44.381619	37.965156	43.595947
79	H	44.693834	39.514853	45.079348
80	C	44.958628	36.917938	42.873358
81	H	46.758417	35.763399	42.559240

82	H	43.337764	38.240396	43.424082
83	H	44.372161	36.359129	42.141476

7. XPS analysis.

All the binding energies were corrected with reference to the C1s peak at 284.8 eV. CasaXPS software was used for peak analysis and de-convolution studies.

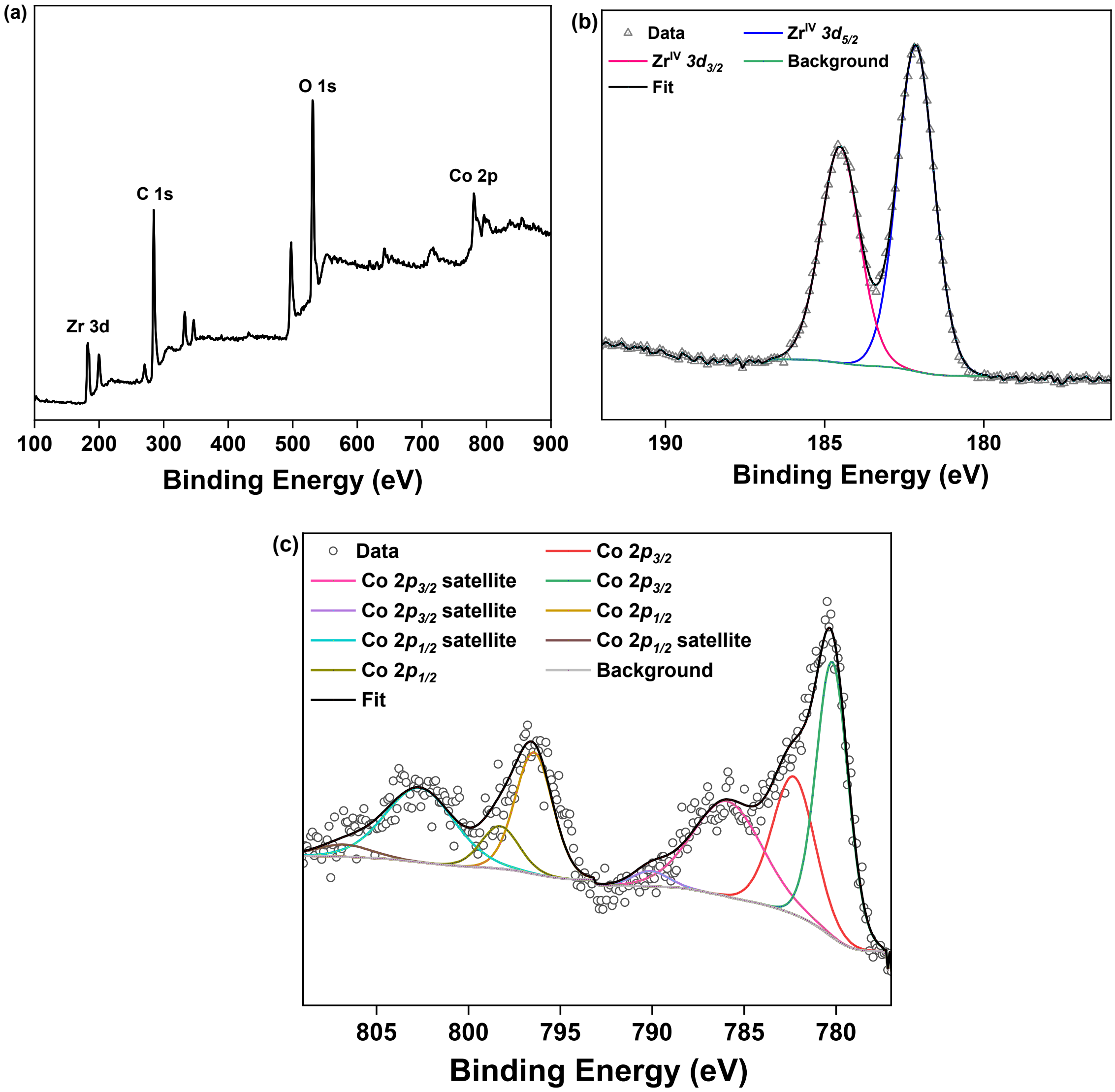

Figure S15. (a) Raw XPS data of UiO-67-CoH before catalysis. (b) XPS fitting of zirconium 3d in UiO-67-CoH before catalysis. (c) XPS fitting of cobalt 2p in UiO-67-CoH before catalysis.

Component	Position (eV)	FWHM (eV)	Area%	Line shape
Co(II) $2p_{3/2}$	780.5	2.0	26.21	GL (30)
Co(II) $2p_{3/2}$	782.06	2.7	17.29	GL (30)
Co(II) $2p_{3/2}$	786.01	4.4	19.63	GL (30)
Co(II) $2p_{3/2}$	790.41	2.3	1.62	GL (30)
Co(II) $2p_{1/2}$	796.12	2.4	13.49	GL (30)

Co(II) *2p1/2*	797.58	2.1	4.72	GL (30)
Co(II) *2p1/2*	802.43	4.4	15.09	GL (30)
Co(II) *2p1/2*	806.32	3.5	1.96	GL (30)

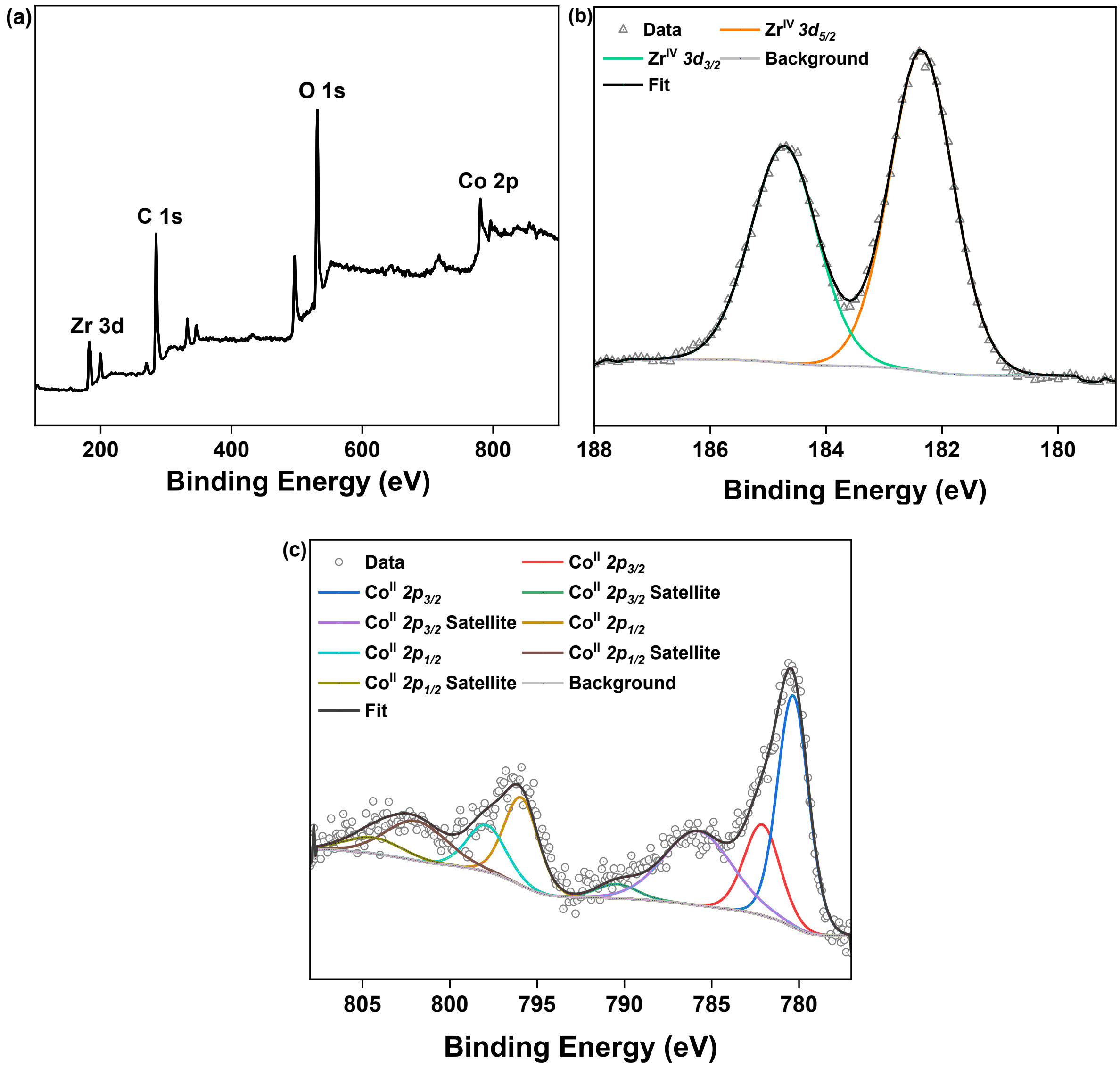

Figure S16. (a) Raw XPS data of UiO-67-Co after catalysis. (b) XPS fitting of zirconium 3d in UiO-67-Co after catalysis. (c) XPS fitting of cobalt 2p in UiO-67-Co after catalysis.

Component	**Position (eV)**	**FWHM (eV)**	**Area%**	**Line shape**
Co(II) *2p3/2*	780.30	2.1	29.90	GL (30)
Co(II) *2p3/2*	782.45	2.4	13.45	GL (30)
Co(II) *2p3/2*	785.92	4.5	20.89	GL (30)

Co(II) $2p_{3/2}$	790.23	2.7	2.38	GL (30)
Co(II) $2p_{1/2}$	796.09	2.3	12.38	GL (30)
Co(II) $2p_{1/2}$	798.10	2.5	7.42	GL (30)
Co(II) $2p_{1/2}$	802.35	4.0	9.88	GL (30)
Co(II) $2p_{1/2}$	806.04	3.79	3.70	GL (30)

8. Characterization of the synthesized *N*-formylated products.

The conversion and the yield for *N*-formylation reactions were determined by Agilent 7890B gas chromatograph equipped with a mass detector (Agilent 5977B GC/MSD) and HP-5MS UltraInert 30m-250µm-0.25µm column for GC-MS with the following chromatographic conditions: He was used as the carrier gas with a flow rate of 1 mL min^{-1}, an injection volume of 5.0 μL, an initial column oven temperature of 100 °C which was gradually increased to 250 °C at a rate of 5 °C min^{-1} and a detector temperature of 250 °C. The conversion of the reactants were analyzed by GC-MS using area-percent method and yield of the products were determined by GC using mesitylene as an internal standard.

Table S8. GC-MS retention time of the *N*-formylated products catalyzed by UiO-67-CoH.

SNo.	Products	GC-MS retention time
1.	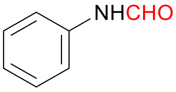	13.03
2.	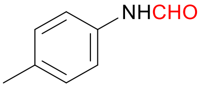	13.64
3.	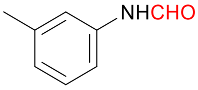	13.06
4.	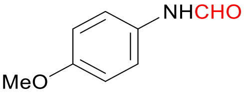	12.79
5.	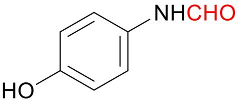	12.46
6.	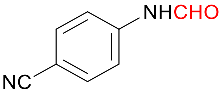	15.36
7.	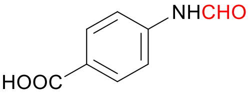	10.92
8.	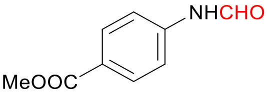	13.28

SNo.	Products	GC-MS retention time
9.	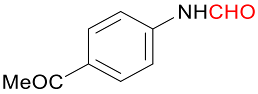	19.21
10.	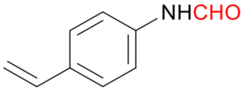	15.23
11.	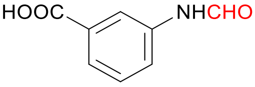	11.05
12.	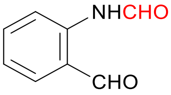	11.49
13.	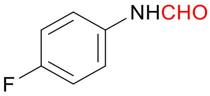	14.66
14.	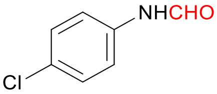	15.21
15.	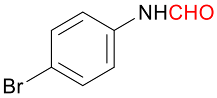	16.80
16.	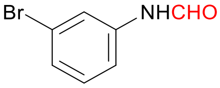	16.59

17.	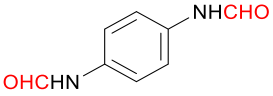	8.95
18.	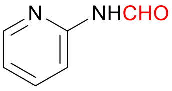	10.76
19.	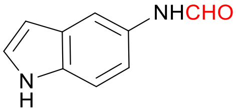	13.21
20.	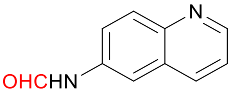	16.32
21.	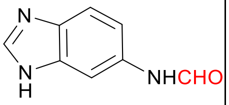	11.28
22.	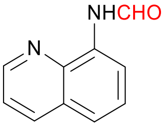	15.91
23.	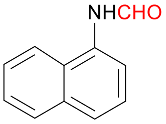	11.68
24.	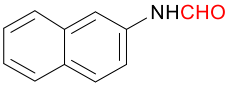	11.11
25.		4.44
26.		5.16
27.	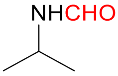	4.89
28.	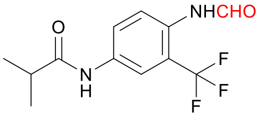	9.76

8.1 NMR data of the *N*-formylated products.

N-Phenylformamide (2a).[13]

^{1}H NMR (400 MHz, $CDCl_3$, ppm): δ 8.63 (d, J = 11.4 Hz, 1H, trans), 8.31 (d, J = 1.2 Hz, 1H, cis), 8.04 (brs, 1H, cis), 7.47 (d, 2H), 7.33-7.23 (m, 4H),7.16-7.05 (m, 2H), 7.04-6.99 (d, 2H). GC-MS: 121.1.

***N-p*-Tolylformamide (2b).**[13]

^{1}H NMR (400 MHz, $CDCl_3$, ppm): δ 8.55 (d, J = 11.5 Hz, 1H, trans), 8.27 (d, J = 1.6 Hz, 0.89H, cis), 8.18 (brs, 0.88H, trans), 7.41 (brs, 0.60H, cis), 7.35 (d, 1.80H), 7.07 (m, 3.67H), 6.91 (d, 1.99H), 2.25 (d, 5.59H). GC-MS: 135.1.

***N-m*-Tolylformamide (2c).**[13]

^{1}H NMR (400 MHz, $CDCl_3$, ppm): δ 8.61 (d, J = 11.4 Hz, 1H, trans), 8.41 (brs, J = 22.3 Hz, 0.88H, trans), 8.28 (d, J = 1.2 Hz, 0.75H, cis), 7.44 (brs, 0.71H, cis), 7.33 (s, 0.74H), 7.24 (d, 0.73H), 7.18-7.10 (m, 1.71H), 6.95 – 6.80 (m, 3.63H), 2.27 (d, 5.13H). GC-MS: 135.1.

***N*-(4-Methoxyphenyl) formamide (2d).**[13]

^{1}H NMR (400 MHz, $CDCl_3$, ppm): δ 8.43 (d, J = 11.5 Hz, 1H, trans), 8.24 (d, J = 1.2 Hz, 1.07H, cis), 7.96 (brs, 0.92H, trans), 7.46-7.32 (m, 3.05H), 7.00-6.91 (m, 2.05H), 6.85-6.74 (m, 4.11H), 3.72 (d, 6.05H). GC-MS: 151.1.

***N*-(4-Hydroxyphenyl) formamide (2e).**[13]

^{1}H NMR (400 MHz, DMSO-*d*$_6$, ppm): δ 9.95-9.79 (m, 1.27H), 9.26 (d, 1.31H), 8.51 (d, J = 11.2 Hz, 0.30H, trans), 8.17 (d, J = 1.9 Hz, 1.00H, cis), 7.38 (m, 1.98H), 7.02-6.94 (m, 0.63H), 6.71 (m, 2.64H). GC-MS:137.1.

***N*-(4-Cyanophenyl) formamide (2f).**[13]

^{1}H NMR (DMSO-*d*$_6$, 500 MHz, ppm): (trans/cis=25/75), δ 10.59 (brs, 1H, cis), 10.47 (d, J = 10.2 Hz, 1H, trans), 8.93 (d, J = 10.5 Hz, 1H, trans), 8.31 (s, 1H, cis), 7.71 (q, J = 8.6 Hz, 2H, trans, 4H, cis), 7.32 (d, J = 7.7 Hz, 2H, trans). GC-MS: 146.1.1

4-Formamidobenzoic acid (2g).[14]

^{1}H NMR (250 MHz, DMSO-*d*$_6$, ppm): δ 12.73 (brs, 1H), 10.66 (s, 1H), 8.32 (s, 1H), 7.84 (d, 2H, J= 6.95, Ar-H), 7.65 (d, 2H, J= 8.67, Ar-H)). GC-MS: 165.1.

Methyl 4-formamidobenzoate (2h).[15]

^{1}H NMR ($CDCl_3$, 500 MHz, ppm): (trans/cis=45/55), δ 9.00 (br s, 1H, trans), 8.82 (d, J = 11.1 Hz, 1H, trans), 8.38 (s, 1H, cis), 8.23 (br s, 1H, cis), 7.98 (d, J = 8.5 Hz, 2H, trans), 7.95 (d, J = 8.6 Hz, 2H, cis), 7.61 (d, J = 8.6 Hz, 2H, cis), 7.12 (d, J = 8.6 Hz, 2H, trans), 3.87 (s, 3H, trans), 3.85 (s, 3H, cis). GC-MS: 179.1.

***N*-(4-Acetylphenyl) formamide (2i).**[15]

^{1}H NMR ($CDCl_3$, 500 MHz, ppm): (trans/cis=35/65), δ 9.36 (d, J = 10.7 Hz, 1H, trans), 8.92 (d, J = 3.9 Hz, 1H, cis), 8.90 (brs, 1H, trans), 8.46 (d, J = 0.9 Hz, 1H, cis), 7.97 (d, J = 8.5 Hz, 2H, trans), 7.93 (d, J = 8.6 Hz, 2H, cis), 7.72 (d, J = 8.6 Hz, 2H, cis), 7.23 (d, J = 8.5 Hz, 2H, trans), 2.60 (s, 3H, trans), 2.59 (s, 3H, cis). GC-MS: 163.1.

N-(4-Vinylphenyl) formamide (2j).[16]

^{1}H NMR (500 MHz, CDCl$_3$, ppm): δ 8.70 (d, J = 11.3 Hz, 1H), 8.37 (s, 1H), 8.24 (brs, 1H), 7.51 (d, J = 7.8 Hz, 2H), 7.39 (t, J = 9.2 Hz, 4H), 7.05 (d, J = 7.7 Hz, 2H), 6.68 (dd, J = 16.1, 12.3 Hz, 2H), 5.70 (dd, J = 17.5, 7.2 Hz, 2H), 5.23 (dd, J = 14.1, 11.3 Hz, 2H). GC-MS: 147.1.

3-Formamidobenzoic acid (2k).[17]

^{1}H-NMR (DMSO-d_6, 400.13 MHz, ppm): δ 10.35 (brs, 1H), 8.32 (d, lH, 1.6 Hz), 8.06 (s, 1H), 7.74 (d, 1H, 7.8 Hz), 7.68 (d, 1H, 7.2 Hz), 7.29 (m, lH). GC-MS: 165.1.

N-(4-Fluorophenyl) formamide (2m).[15]

^{1}H NMR (CDCl$_3$, 500 MHz, ppm): (trans/cis=40/60), δ 8.58 (d, J = 11.3 Hz, 1H, trans), 8.36 (s, 1H, cis), 8.13 (br s, 1H, trans), 7.51 (dd, J = 9.0, 4.7 Hz, 2H, cis), 7.36 (br s, 1H, cis), 7.07 (d, J = 6.1 Hz, 4H, trans), 7.03 (t, J = 8.6 Hz, 2H, cis). GC-MS: 139.1.

N-(4-Chlorophenyl) formamide (2n).[15]

^{1}H NMR (CDCl$_3$, 500 MHz, ppm): (trans/cis=40/60), δ 8.66 (d, J = 10.6 Hz, 1H, trans), 8.61 (br s, 1H, trans), 8.36 (s, 1H, cis), 7.66 (br s, 1H, cis), 7.50 (d, J = 8.7 Hz, 2H, cis), 7.33 (d, J = 8.6 Hz, 2H, trans), 7.29 (d, J = 8.7 Hz, 2H, cis), 7.04 (d, J = 8.6 Hz, 2H, trans). GC-MS: 155.5.

N-(4-Bromophenyl) formamide (2o).[13]

^{1}H NMR (400 MHz, CDCl$_3$, ppm) δ 8.59 (d, J = 11.2 Hz, 0.74H, trans), 8.49 (brs, 0.64H, trans), 8.30 (s, 1H, cis), 7.56 (brs, 0.91H, cis), 7.43-7.32 (m, 5.43H), 6.91 (d, 1.44H). GC-MS: 200.0.

N-(3-Bromophenyl) formamide (2p).[13]

^{1}H NMR (400 MHz, CDCl$_3$, ppm): δ 8.62 (d, J = 11.1 Hz, 0.83H, trans), 8.57 (brs, 0.67H, trans), 8.29 (d, J = 1.2 Hz, 1H, cis), 7.73 (t, J = 1.8 Hz, 1.01H), 7.64 (brs, 0.85H, cis), 7.38 (d, J = 8.0 Hz, 1.01H), 7.28-7.20 (m, 1.9H), 7.19-7.08 (m, 2.37H), 6.97 (dd, 0.80H). GC-MS: 200.0.

N,N′-(1,4-Phenylene) diformamide (2q).[18]

^{1}H NMR (400Hz, (CD$_3$)$_2$SO, ppm): δ 10.14-10.06 (m, 2.00H), 8.69 (minor rotamer, d, J = 11.2 Hz, 0.46H), 8.23 (major rotamer, d, J = 1.6 Hz, 1.54H), 7.54-7.52 (m, 3.10H), 7.15-7.13 (m, 0.90H). GC-MS: 164.1.

N-(pyridin-2-yl) formamide (2r).[18]

^{1}H NMR (400 MHz, $CDCl_3$, ppm): *δ* 10.30 (minor rotamer, brs, 0.41H), 10.11 (major rotamer, br s, 0.59H), 9.34 (minor rotamer, d, J = 10.4 Hz, 0.43H), 8.55 (major rotamer, s, 0.57H), 8.35 (d, J = 4.4 Hz, 1.00H), 8.28 (d, J = 8.4 Hz, 0.57H), 7.76 (t, J = 7.8 Hz, 0.57H), 7.69 (t, J = 7.8 Hz, 0.43H), 7.13-7.07 (m, 1.00H), 6.95 (d, J = 8.0 Hz, 0.43H). GC-MS: 122.1.

***N*-(1H-Indol-5-yl) formamide (2s).**[18]

^{1}H NMR (400 MHz, $(CD_3)_2CO$, ppm): *δ* 10.28 (major rotamer, br, 0.52H), 9.19 (minor rotamer, s, 0.48H), 8.69-8.66 (m, 0.30H), 8.36 (major rotamer, s, 0.70H), 8.18 (br d, J = 11.6 Hz, 0.27H), 8.04 (s, 0.63H), 7.44-7.32 (m, 2.88H), 7.02 (dd, J = 8.6, 1.8 Hz, 0.32H), 6.46-6.44 (m, 0.90H), 3.17 (s, 16 0.79H). GC-MS: 160.1.

***N*-(Quinolin-6-yl) formamide (2t).**[13]

^{1}H NMR (400 MHz, DMSO-*d*$_6$, ppm): δ 10.55 (s, 0.74H, cis), 10.48 (d, J = 10.8 Hz, 0.24H, trans), 8.99 (d, J = 10.8 Hz, 0.24H, trans), 8.79 (dd, J = 4.1, 1.6 Hz, 1H, cis), 8.40 (dd, 1.66H), 8.32-8.11 (m, 1.28H), 7.99 (d, 1.02H), 7.79 (dd, 0.81H), 7.76-7.61 (m, 0.56H), 7.52-7.43 (m, 1.02H). GC-MS: 172.1.

***N*-(8-Quinolinyl) formamide (2v).**[18]

^{1}H NMR (400 MHz, $CDCl_3$, ppm): *δ* 9.81 (major rotamer, s, 0.79H), 9.47 (minor rotamer, br s, 0.10H), 9.14 (minor rotamer, d, J = 12.0 Hz, 0.11H), 8.83 (d, J = 4.0 Hz, 0.99H), 8.78-8.74 (m, 0.87H), 8.71 (major rotamer, s, 0.89H), 8.19 (d, J = 8.0 Hz, 0.99H), 7.59-7.47 (m, 3.13H). GC-MS:

***N*-(Naphthalen-1-yl) formamide (2w).**[18]

^{1}H NMR (400 MHz, $CDCl_3$, ppm): *δ* 8.90 (major rotamer, d, J = 8.8 Hz, 0.67H), 8.64 (major rotamer, d, J = 10.8 Hz, 0.75H), 8.61 (br s, minor rotamer, 0.25H), 8.04 (d, J = 8.0 Hz, 0.74H, HAr), 8.00 (d, J = 7.6 Hz, 0.29H), 7.91-7.78 (m, 2.32H), 7.71 (d, J = 8.0 Hz, 0.28H), 7.61-7.50 (m, 2.05H), 7.46 (t, J = 8.0 Hz, 1.05H), 7.31 (d, J = 7.2 Hz, 0.72H). GC-MS: 171.1.

***N*-(Naphthalene-2-yl) formamide (2x).**[18]

^{1}H NMR (400 MHz, $(CD_3)_2SO$, ppm): *δ* 10.45-10.40 (m, 0.98H), 8.98 (minor rotamer, d, J = 10.8 Hz, 0.24H), 8.41 (major rotamer, s, 0.76H), 8.34 (s, 0.74H), 7.88-7.78 (m, 3.02H), 7.69 (s, 0.25H), 7.59 (d, J = 8.8 Hz, 0.75H), 7.49-7.38 (m, 2.22H). GC-MS: 171.1.

N-Ethyl formamide (2y).[18]

^{1}H NMR (CDCl$_3$, 500 MHz, ppm): (trans/cis=15/85), δ 8.11 (s, 1H, cis), 8.05 (d, J = 12.1 Hz, 1H, trans), 7.10 (br s, 1H, cis), 6.78 (br s, 1H, trans), 3.34-3.29 (m, 2H, cis), 3.27 (dd, J = 9.4, 4.3 Hz, 2H, trans), 1.21 (t, J = 7.2 Hz, 3H, trans), 1.17 (t, J = 7.3 Hz, 3H, cis). GC-MS: 73.0.

N-Propyl formamide (2z).[19]

^{1}H NMR (501 MHz, DMSO-d$_6$, ppm): δ 7.90 (s, 1H), 3.43 (s, 1H), 2.93 (d, J = 3.9 Hz, 2H), 1.31 (d, J = 10.6 Hz, 2H), 0.74 (d, J = 10.7 Hz, 3H). GC-MS: 87.1.

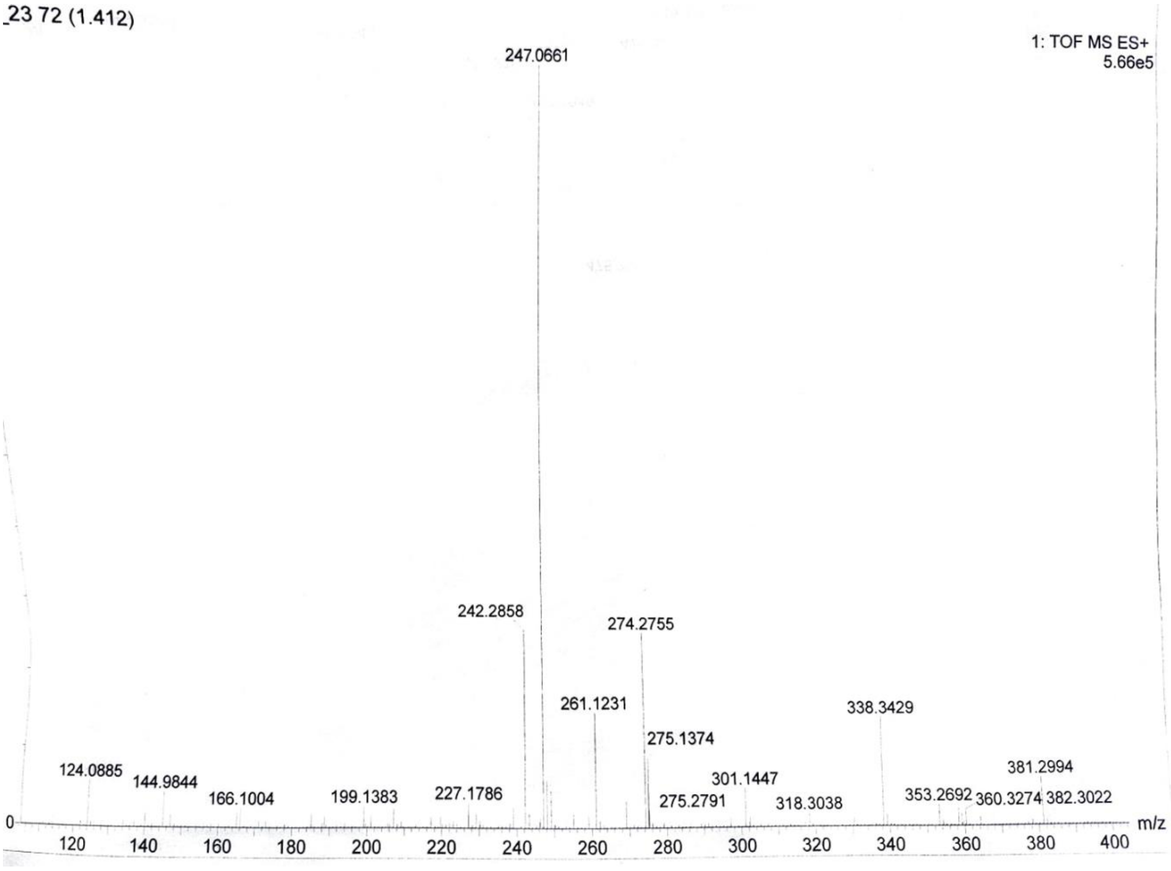

Figure S17. HRMS spectrum of PhH$_2$SiO-SiH(OH)Ph. HRMS (ESI) m/z: calcd for C$_{12}$H$_{15}$O$_2$Si [M+H]$^+$ 247.0611; found 247.0661.

(a)

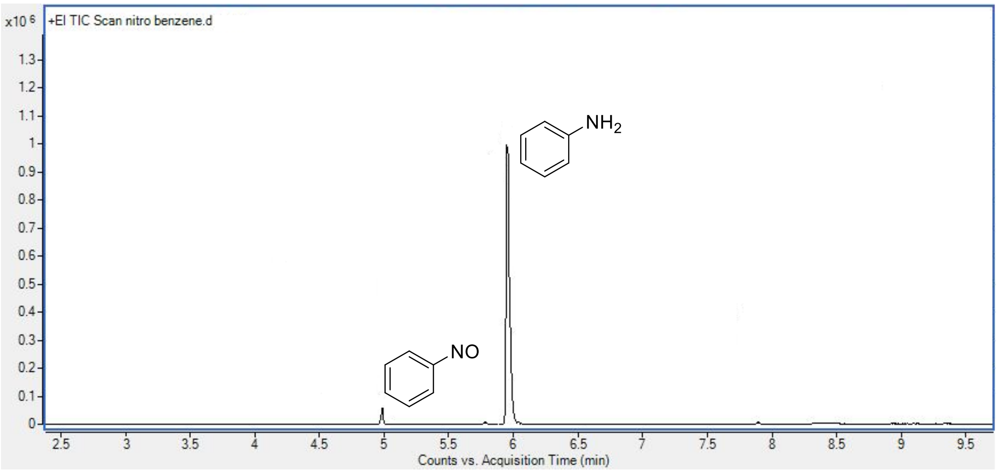

(b)

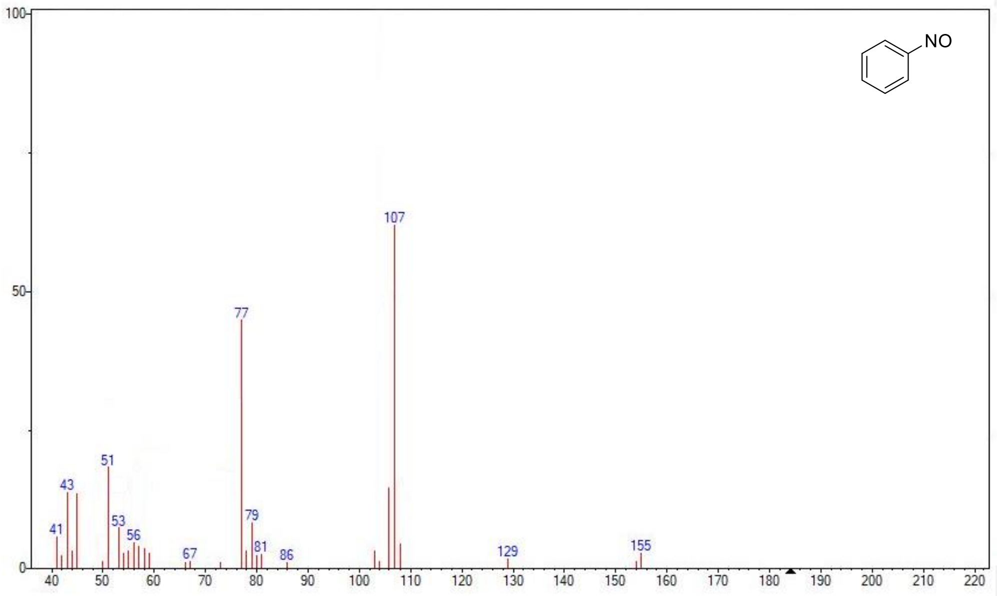

Figure S18. GC-MS spectra of the catalytic *N*-formylation of nitrobenzene mediated by UiO-67-CoH. Reaction conditions: UiO-67-CoH (4 mg, 0.25 mol% Co), 2.5 equiv. $PhSiH_3$, 10 bar CO_2, 3.0 mL THF, 120 °C for 10 h. The chromatographic peak at a retention time (RT) of 4.912 min corresponds to the nitrosobenzene intermediate generated in situ during the catalytic *N*-formylation reaction.

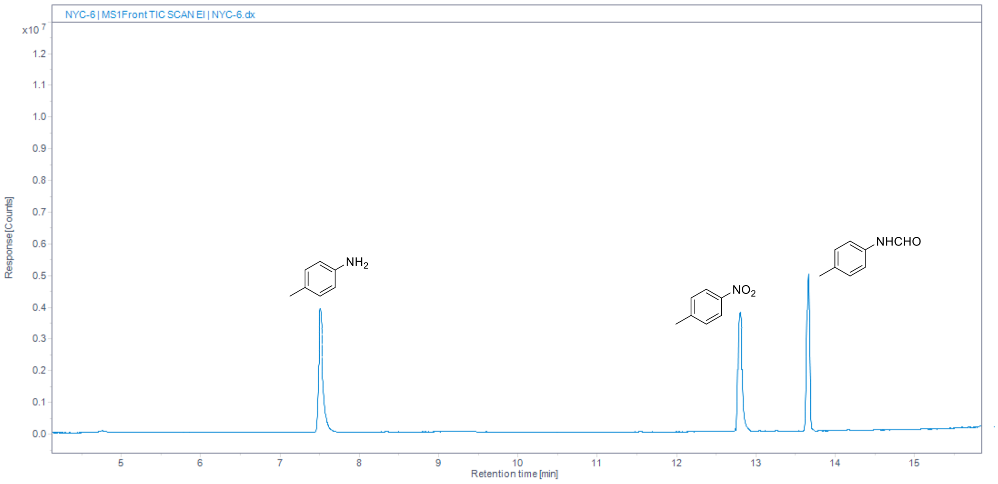

Figure S19. GC-MS spectra of the catalytic *N*-formylation of *p*-nitrotolune mediated by UiO-67-CoH. Reaction conditions: UiO-67-CoH (4 mg, 0.25 mol% Co), 2.5 equiv. $PhSiH_3$, 5 bar CO_2, 3.0 mL THF, 120 °C for 36 h.

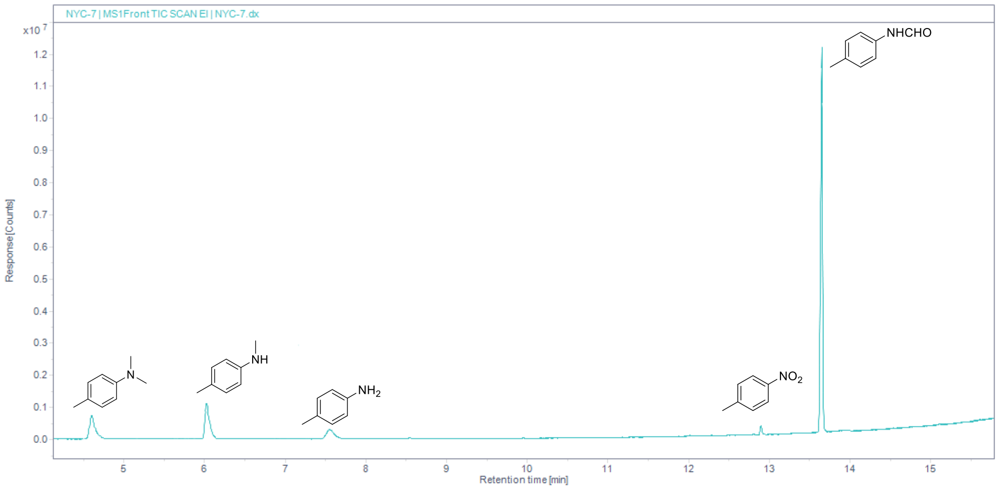

Figure S20. GC-MS spectra of the catalytic *N*-formylation of *p*-nitrotolune mediated by UiO-67-CoH. Reaction conditions: UiO-67-CoH (4 mg, 0.25 mol% Co), 2.5 equiv. $PhSiH_3$, 15 bar CO_2, 3.0 mL THF, 120 °C for 36 h.

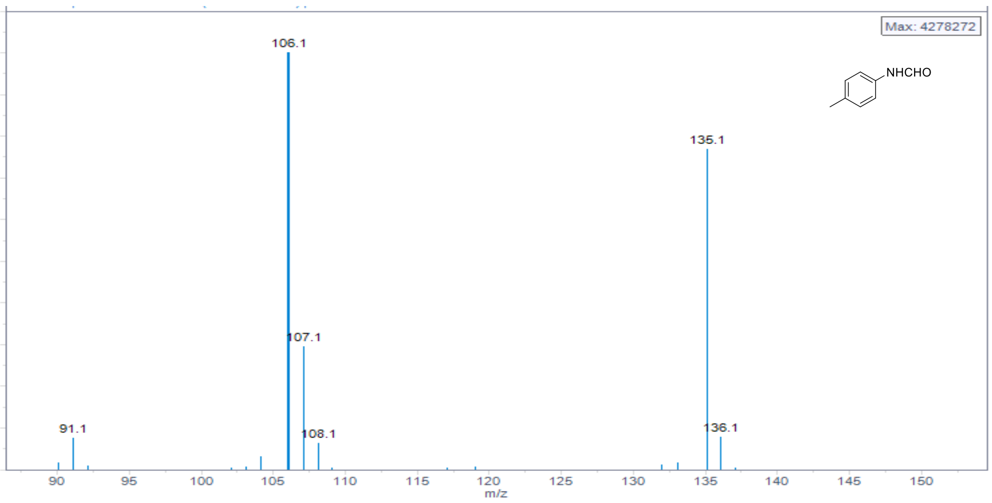
Max: 4278272
NHCHO
106.1
135.1
107.1
108.1
91.1
136.1
90
95
100
105
110
115
120
125
130
135
140
145
150
m/z

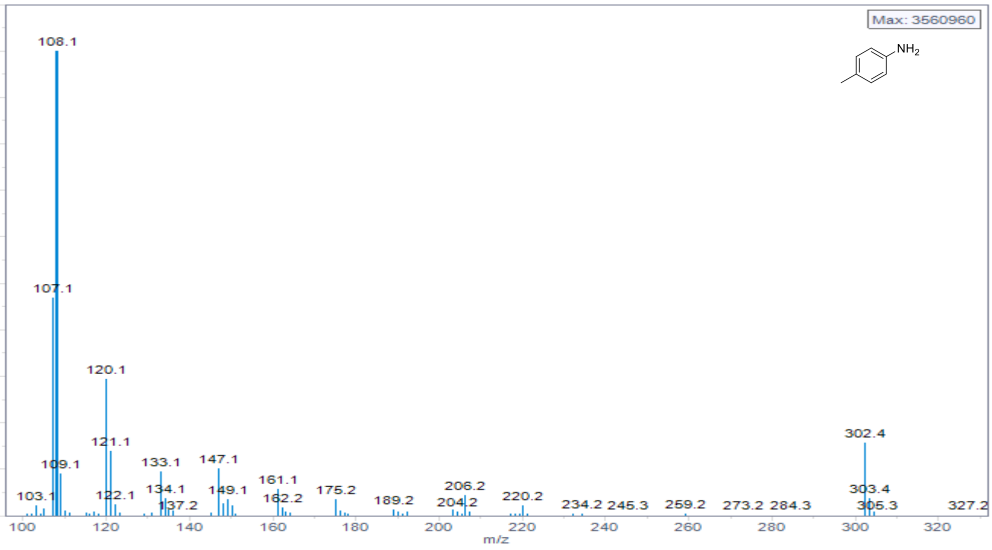
Max: 3560960
NH_2
108.1
107.1
120.1
121.1
109.1
133.1
147.1
161.1
103.1
122.1
134.1
137.2
149.1
162.2
175.2
189.2
206.2
204.2
220.2
234.2
245.3
259.2
273.2
284.3
302.4
303.4
305.3
327.2
100
120
140
160
180
200
220
240
260
280
300
320
m/z

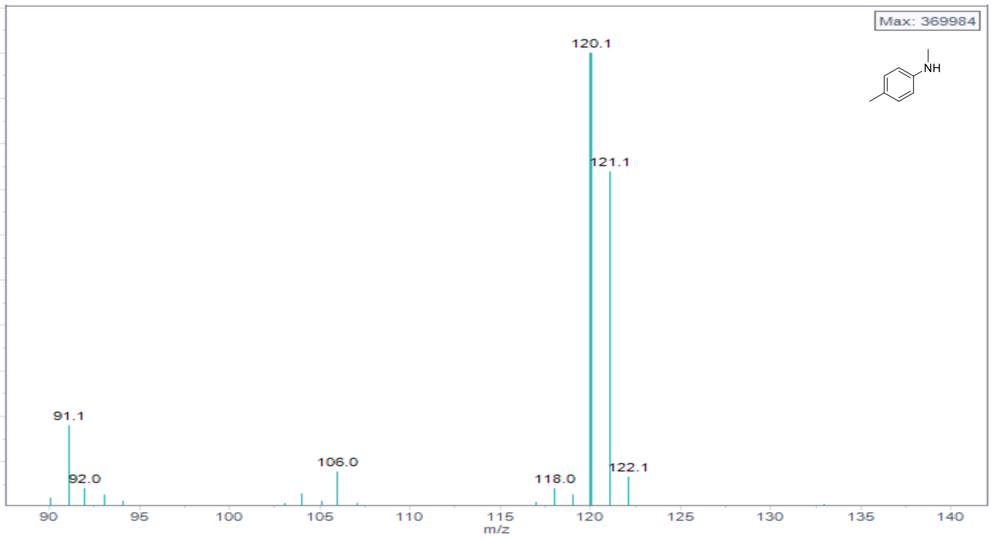
Max: 369984
NH
120.1
121.1
91.1
92.0
106.0
118.0
122.1
90
95
100
105
110
115
120
125
130
135
140
m/z

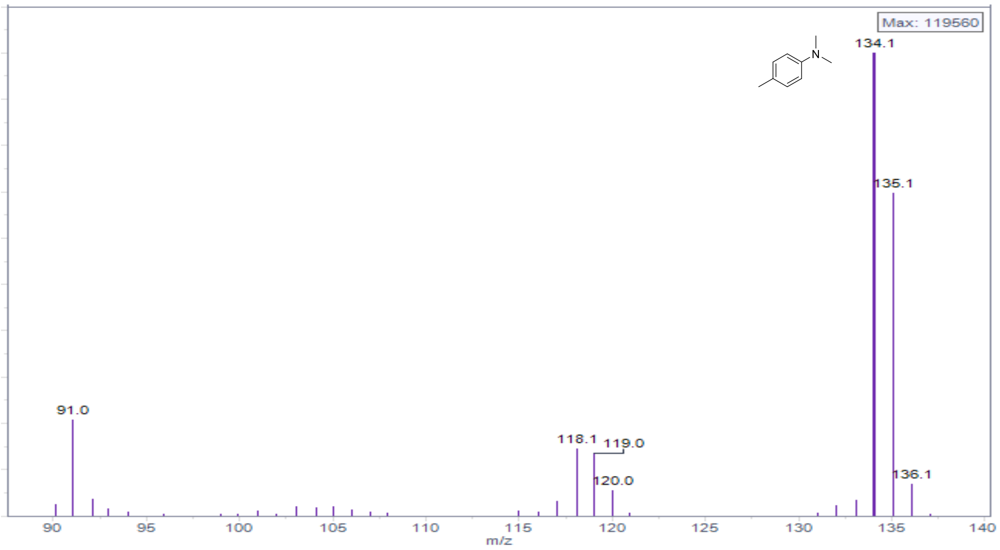
Max: 119560
N
134.1
135.1
91.0
118.1
119.0
120.0
136.1
90
95
100
105
110
115
120
125
130
135
140
m/z

Table S9. Comparison of the catalytic activity of UiO-67-CoH with that of other reported catalysts in *N*-formylation of nitro compounds.

SNo.	**Reference**	**Catalyst**	**Conditions**	**C1 source**	**%Yield of *N*-formylated products**
1.	*Green Chem.*, **2016**, 18, 1019-1022	AgPd@g-C_3N_4	25 mg catalyst/1mmol nitro substrate/1 mL H_2O/40-watt bulb/2 h	HCOOH (2 mmol)	75-99
3.	*Adv. Synth.Catal.*, **2017**, 360, 432-437	Pd@PS (8 mol% Pd)	0.73 mmol nitro substrate/3 mL DMF/408 K/20 h	$HO_2CCO_2H.2 H_2O$ (11 mmol)	76-89
4.	*Chem. Commun.,* **2018**, 54¸ 8913-8916	Co@NPC-800	20 mg catalyst/0.25 mmol nitro substrate/2.5 mL THF/393 K/12 h	$HCOONH_4$ (25 mmol)	46-98
5.	*Catal. Commun.,* **2019**¸ 129, 105747	CoNC-700	9.5 mg catalyst/0.5 mmol nitro substrate/5 mL ACN/1 bar N_2/110 °C/2 h	HCOOH (5 mmol)	20-95
6.	*ChemCatChem*, **2020**, 12, 1546-1550	ZnNC-1000 (3 mol% Zn)	20 mg catalyst/ 0.5 mmol nitro substrate/2 mL THF/423 K/16 h	HCOOH (3 mmol)	96
7.	*Chem. Commun.,* **2020***,* 56, 9620-9623	Fe nano powder	1 mmol catalyst/0.5 mmol nitro substrate/ 1 mmol TMDSO/0.05 mmol KI/1.5 mL DMF/135 °C/28 h	CO_2 balloon	45-85
8.	*ChemCatChem*, **2021**, 13, 3174-3183	ZnCo-N@C(ZIF-COF)	30 mg catalyst/1 mmol nitro substrate/7 mL THF/413 K/8 h	HCOOH (12 mmol)	78-93
9.	*ACS Appl. Mater. Interfaces*, **2022**, 14, 55568-55576	Mn1-N/P-C	20 mg catalyst/0.5 mmol nitro substrate/THF: H_2O (1.5:0.5 mL)/393 K/12 h	HCOOH (3 mmol)	40-99
10.	*ACS Appl. NanoMater.,*	Pd 1.5%/Ti-MOF	30 mg photocatalyst/0.3 mmol nitro	HCOOH (8 equiv.)	92

	2022, 5, 464−475		substrate/3mL H_2O/6 h/whiteLED(5W×4).		
11.	*ACS Catal.* **2023**, 13, 8372-8383	ZrO_2/C@1.0-Co-NC	40 mg catalyst/ 1.0 mmol nitro substrate/6.0 mmol Ph_2SiH_2/2 mL DMF/ 60 °C/24 h	1 atm CO_2	87-99
12.	*J.Catal.,* **2024**, 440*,* 115826	meso-phen-900	50 mg catalyst/0.5 mmol nitro substrate/ 2 mL toluene/ 0.1 MPa N_2/ 120 °C/12 h	HCOOH (2.5 mmol)	60-89
13.	*Molecular Catalysis*, **2025**, 572, 114792	1.0% Co-NPs/NC	10 mg catalyst/0.5 mmol nitro substrate /3 mL toluene/373 K/5 h	HCOOH (5 mmol)	99
14.	*ACS Sustainable Chem. Eng.* **2025***,* 13, 40, 16971–16980	20 mol % $TiCp_2Cl_2$	24.8mg catalyst/0.5 mmol nitro substrate/2 equiv. NaOMe/ 5 equiv. $NH_3\cdot BH_3$/ 5 mL of MeCN/ 100 °C/48 h	10 bar CO_2	54-78
15.	**This Work**	**UiO-67-CoH (0.75 mol% Co)**	**12 mg catalyst/1.3 mmol nitro substrate/ 2.5 equiv. of $PhSiH_3$/ 3.0 mL THF/120 °C, 36 h**	**10 bar CO_2**	**55-94**

9. References.

1 J. H. Cavka, S. Jakobsen, U. Olsbye, N. Guillou, C. Lamberti, S. Bordiga and K. P. Lillerud, *J. Am. Chem. Soc.*, 2008, **130**, 13850–13851.
2 Y. Bai, Y. Dou, L.-H. Xie, W. Rutledge, J.-R. Li and H.-C. Zhou, *Chem. Soc. Rev.*, 2016, **45**, 2327–2367.
3 D. Kowalkowska-Zedler, N. Nedelko, K. Kazimierczuk, P. Aleshkevych, R. Łyszczek, A. Ślawska-Waniewska and A. Pladzyk, *RSC Adv.*, 2020, **10**, 29100–29108.
4 J. Yang, H.-Q. Chen, N. Shi, T. Wang, J. Liu and W.-P. Pan, *Chem. Eng. J.*, 2022, **428**, 132095.
5 A. K. Poswal, A. Agrawal, A. K. Yadav, C. Nayak, S. Basu, S. R. Kane, C. K. Garg, D. Bhattachryya, S. N. Jha and N. K. Sahoo, N. K. Commissioning and First Results of Scanning Type EXAFS Beamline (BL-09) at INDUS-2 synchrotron source. *AIP Conf. Proc.* 2014, **1591**, 649–651.
6 B. Ravel and M. Newville, *J. Synchrotron Radiat.*, 2005, **12**, 537–541.
7 M. Araújo, B. Lasorne, A. L. Magalhães, G. A. Worth, M. J. Bearpark and M. A. Robb, *J. Chem. Phys.*, 2009, **131**, 144301.
8 V. Yempally, S. J. Kyran, R. K. Raju, W. Y. Fan, E. N. Brothers, D. J. Darensbourg and A. A. Bengali, *Inorg. Chem.*, 2014, **53**, 4081–4088.
9 P. Bhumla, M. Kumar and S. Bhattacharya, *Nanoscale Adv.*, 2021, **3**, 575–583.
10 S. Impeng, S. Siwaipram, S. Bureekaew and M. Probst, *Phys. Chem. Chem. Phys.*, 2017, **19**, 3782–3791.
11 S. Canneaux, F. Bohr and E. Henon, *J. Comput. Chem.*, 2014, **35**, 82–93.

12 E. R. Johnson and A. D. Becke, *J. Chem. Phys.*, 2006, **124**, 174104.
13 X. Dong, Z. Wang, Y. Duan and Y. Yang, *Chem. Commun.*, 2018, **54**, 8913–8916.
14 M. Hosseini-Sarvari and H. Sharghi, *J. Org. Chem.*, 2006, **71**, 6652–6654.
15 L. Yu, Q. Zhang, S. Li, J. Huang, Y. Liu, H. He and Y. Cao, *ChemSusChem*, 2015, **8**, 3029–3035.
16 M. Jia, H. Zhang, Y. Lin, D. Chen, Y. Chen and Y. Xia, *Org. Biomol. Chem.*, 2018, **16**, 3615–3624.
17 A. Syahrani, T. S. Panjaitan, G. Indrayanto and A. L. Wilkins, *J. Asian Nat. Prod. Res.*, 2000, **2**, 305–309.
18 J. Yin, J. Zhang, C. Cai, G.-J. Deng and H. Gong, *Org. Lett.*, 2019, **21**, 387–392.
19 D. Dan, F. Chen, W. Zhao, H. Yu, S. Han and Y. Wei, *Dalton Trans.*, 2021, **50**, 90–94.